FIG. 5. **Immunohistochemical analysis with an anti-HDC antibody in the testis of W/W$^+$ and W/W^V mice.** The testes of W/W$^+$ and W/W^V mice (9–10 weeks of age) were collected, and immunohistochemical analysis was performed with an anti-HDC antibody (1:200) as described in the legend to Fig. 2. *Bar*, 100 μm.

bands were detected in the presence of an excess amount of the antigen, glutathione *S*-transferase fusion HDC (data not shown).

Absence of HDC in the Seminiferous Tubules of W/W^V Mice—W/W^V mice, which are genetically defective in c-Kit (stem cell factor receptor) function, have been reported to lack a significant proportion of their male germ cells. No immunoreactive cells were observed in the seminiferous tubules of W/W^V mice when immunostained with an anti-HDC antibody. On the other hand, a similar staining pattern to that of ICR mice was observed in the testis of W/W$^+$ mice (Fig. 5). Neither HDC activity nor histamine was detectable in the testis of W/W^V mice. In the epididymis, W/W^V mice showed a much lower HDC activity and histamine content than the W/W$^+$ mice (Table II).

Histamine Release Induced by an in Vitro Acrosome Reaction—In vitro acrosome reactions were performed using a calcium ionophore, A23187. Spermatozoa obtained from the cauda epididymis of ICR mice underwent acrosome reactions upon the addition of A23187. Intracellular histamine was completely lost during the reaction for 1 h and about 25% of the histamine was recovered in the medium (Table III). The addition of a diamine oxidase inhibitor, aminoguanidine, had no effect on the recovery of histamine (data not shown).

TABLE II

HDC activity and histamine content in the testis and epididymis of W/W$^+$ and W/W^V mice

The testes and epididymides of each mouse were homogenized and subjected to the assay for HDC activity and histamine as described under "Experimental Procedures." Data are represented as the means ± S.E. (n = 7).

	HDC activity		Histamine	
	Testis	Epididymis	Testis	Epididymis
	fmol/min/mg protein		*pmol/mg protein*	
W/W$^+$	98.9 ± 10.0	22.9 ± 2.50	9.58 ± 0.880	46.7 ± 3.84
W/W^V	<1.00	2.00 ± 2.00[a]	<0.25	3.33 ± 1.76[a]

[a] $p < 0.01$ by Student's t test.

TABLE III

Histamine release by the acrosome reaction induced by A23187

Spermatozoa were collected from the cauda epididymis in the fertilization medium. The acrosome reaction was induced by the addition of a calcium ionophore, A23187 (10 μM) as described under "Experimental Procedures." Histamine content in the A23187-treated spermatozoa and in the medium was measured. Data are represented as the means ± S.E. (n = 3).

	Histamine	
	None	+A23187
	pmol/10^7 cells	
Spermatozoa	14.3 ± 3.31	<0.500
Medium	<0.500	3.40 ± 0.270

DISCUSSION

The abundant expression of HDC mRNA was demonstrated in the mouse testis by Northern blot analysis. Since the function of histamine in the male reproductive system remains to be clarified, our current studies were performed to analyze the possible functions. HDC mRNA and protein were detected in the cells inside the seminiferous tubules. The most intense immunoreactive signals were found in the acrosomes of elongating spermatids. Since immature acrosomes of the round spermatids were also immunoreactive to the anti-HDC antibody, HDC protein expression in the seminiferous tubules may be synchronized with acrosome development. HDC mRNA was also detected by *in situ* hybridization in the cells located near the basement membranes of the seminiferous tubules, which were not immunoreactive to the anti-HDC antibody. Although we were unable to identify which types of cells near the basement membrane were positive upon *in situ* hybridization, these observations suggest that the expression of HDC in these cells may be regulated at the post-transcriptional level.

W/W^V mice, which possess a point mutation in the kinase domain of c-Kit (SCF receptor), are known to be sterile and to lack a significant portion of their germ cells in the seminiferous tubules (10). Studies with a monoclonal antibody, ACK-2, which blocks binding of SCF to c-Kit, have indicated that the SCF/c-Kit interaction is essential for the proliferation of type A spermatogonia in a normal genetic background (23, 24). W/W^V mice are known to lack spermatocytes, spermatids, and spermatozoa. The absence of the HDC protein in the seminiferous tubules and the lack of enzymatic activity in the testis of W/W^V mice is consistent with the observation that HDC is selectively expressed in the spermatids and spermatozoa. The relationship between membrane-bound SCF expression in Sertoli cells and c-Kit expression in male germ cells (spermatogonia and spermatids) is analogous to that between SCF in fibroblasts and c-Kit in immature mast cells. W/W^V mice are also known to lack peripheral mature mast cells, indicating that the SCF/c-Kit signaling is also essential for the development of peripheral mast cells (10). The treatment of interleukin-3-dependent bone marrow-derived mast cells with SCF has been reported to enhance the synthesis of histamine in these cells (7). The acrosome is believed to be analogous to the lysosome (25) and contains a large array of hydrolyzing enzymes such as acrosin and hyaluronidase (26). We previously demonstrated that HDC is localized in the granular fraction of a rat mast cell line, RBL-2H3 (5). Male germ cells and mast cells may share a common mechanism, a SCF/c-Kit signaling pathway, that may induce the expression and determine the intracellular localization of HDC.

We previously reported that HDC is translated as a 74-kDa precursor and processed into a mature 53-kDa form in a mast cell line (5). The reported molecular mass of purified enzymes from various mammalian tissues has all been 53–55-kDa (19, 20, 27) while the mouse HDC cDNA codes a protein with a predicted molecular mass of 74 kDa (28). Immunoblot analyses demonstrated that different forms of HDC (69, 45, 39, and 35

kDa) are expressed in the male reproductive tissues. We recently generated a mouse strain, genetically lacking the pyridoxal-binding site of HDC, and exhibiting no HDC activity (29, 30). In this strain, no immunoreactive bands were observed in the testis, epididymis, and epididymal spermatozoa (data not shown). Since no splice variants of HDC were detected in the testis by RT-PCR (data not shown), these multiple forms of HDC may be generated by post-translational processing. It is possible that sperm-specific forms of HDC may be produced by a different processing pathway from that in mast cells, since acrosomes are known to contain various specific proteases. A previous study has suggested the existence of a testis-specific form of the c-Kit protein (31). In rat stomach, the existence of multiple forms of HDC have also been reported, where small forms of HDC (40 and 36 kDa) were found to be increased upon the refeeding of fasted rats (32, 33). Since the specific activity of these forms remains to be determined both in the rat stomach and in our study, it is unclear whether these small forms of HDC possess the enzymatic activity. However, since Engel *et al.* (34) have reported that the deletion of the amino-terminal 68 residues and the carboxyl-terminal 20-kDa region has no effect on the K_m value and enzymatic activity of rat HDC, it is possible that the small forms of HDC (39 and 35 kDa) in spermatozoa exhibit enzymatic activity.

In this study, we demonstrated the release of histamine from spermatozoa by an *in vitro* acrosome reaction induced by a calcium ionophore, A23187. Accumulating evidence suggests that fertilizing spermatozoa do not initiate the acrosome reaction *in vivo* until they come into contact with the zona pellucida (14). Although the acrosome reaction induced by a calcium ionophore may be quite different from the zona-induced reaction, it is generally believed that the differences most probably occur during the initial steps of the reaction and not in the downstream cascade of events that occur.

Although a function for histamine in fertilization has not been reported, our results suggest that histamine release may have some function in the fertilization process. We have observed normal fertility in the HDC-deficient mice (29), indicating that histamine production may not be essential in fertility. We are now investigating of male germ cell function and morphology using this mutant mouse strain. To clarify the mechanism as to how histamine modulates the process of fertilization, further experiments, such as *in vitro* fertilization, are surely required.

The recovery of released histamine was quite low in our *in vitro* acrosome reactions. Since the addition of a diamine oxidase inhibitor, aminoguanidine, did not increase the recovery of histamine, the other histamine-metabolizing enzyme, histamine *N*-methyltransferase, may be involved in the degradation of histamine. We have not been able to perform further studies on this point, since we could not obtain a specific inhibitor of histamine *N*-methyltransferase. The expression of diamine oxidase and histamine *N*-methyltransferase in spermatozoa remains unknown.

In summary, we have demonstrated for the first time that there is significant expression of HDC in the spermatids and spermatozoa of male mice and that the release of histamine from spermatozoa can be induced by an *in vitro* acrosome reaction. Our results raise the possibility that histamine may play a role in the mouse reproductive system.

REFERENCES

1. Beaven, M. A. (1978) in *Histamine: Its Role in Physiological and Pathological Processes*, pp. 1–113, Karger, Basel
2. Code, C. F. (1965) *Fed. Proc.* **24,** 1311–1321
3. Schwartz, J. C., Pollard, H., and Quach, T. T. (1980) *J. Neurochem.* **35,** 26–33
4. Tanaka, S., Nemoto, K., Yamamura, E., Ohmura, S., and Ichikawa, A. (1997) *FEBS Lett.* **471,** 203–207
5. Tanaka, S., Nemoto, K., Yamamura, E., and Ichikawa, A. (1998) *J. Biol. Chem.* **273,** 8177–8182
6. Metcalfe, D. D., Baram, D., and Mekori, Y. A. (1997) *Physiol. Rev.* **77,** 1033–1079
7. Lukacs, N. W., Kunkel, S. L., Strieter, R. M., Evanoff, H. L., Kunkel, G., Key, M. L., and Taub, D. D. (1996) *Blood* **87,** 2262–2268
8. Loveland, K. L., and Schlatt, S. (1997) *J. Endocrinol.* **153,** 337–344
9. Kissel, H., Timokhina, I., Hardy, M. P., Rothschild, G., Tajima, Y., Soares, V., Angeles, M., Whitlow, S. R., Manova, K., and Besmer, P. (2000) *EMBO J.* **19,** 1312–1326
10. Russell, E. S. (1979) *Adv. Genet.* **20,** 357–459
11. Reith, A. D., and Bernstein, A. (1991) in *Genome Analysis*, Vol. 3, pp. 105–131, Cold Spring Harbor Laboratory, Cold Spring Harbor, NY
12. Yarden, Y., Kuang, W. J., Yang-Feng, T., Coussens, L., Munemistu, S., Dull, T. J., Chen, E., Schlessinger, J., Francke, U., and Ullrich, A. (1987) *EMBO J.* **6,** 3341–3351
13. Breil, J. D. (1991) in *Elements of Mammalian Fertilization*, Vol. 1 (Wassarman, P. M., ed) pp. 133–151, CRC Press, Inc., Boca Raton, FL
14. Yanagimachi, R. (1994) in *The Physiology of Reproduction* (Knobil, E., and Neil, J. D., ed) pp. 189–317, Raven, New York
15. Sugimoto, Y., Namba, T., Shigemoto, R., Negishi, M., Ichikawa, A., Narumiya, S. (1994) *Am. J. Physiol.* **266,** F823–F828
16. Asahara, M., Mushiake, S., Shimada, S., Fukui, H., Kinoshita, Y., Kawanami, C., Watanabe, T., Tanaka, S., Ichikawa, A., Uchiyama, Y., Narushima, Y., Takasawa, S., Okamato, H., Tohyama, M., and Chiba, T. (1996) *Gastroenterology* **111,** 45–55
17. Shore, P. A., Burkhalter, A., and Cohn, V. H. (1959) *J. Pharmacol. Exp. Ther.* **127,** 182–186
18. Bradford, M. M. (1974) *Anal. Biochem.* **72,** 248–254
19. Ohmori, E., Fukui, T., Imanishi, N., Yatsunami, K., and Ichikawa, A. (1990) *J. Biochem. (Tokyo)* **107,** 834–839
20. Yamamoto, J., Fukui, T., Suzuki, K., Tanaka, S., Yatsunami, K., and Ichikawa, A. (1993) *Biochim. Biophys. Acta* **1216,** 431–440
21. Whittingham, D. G. (1968) *Nature* **220,** 592–593
22. Watanabe, T., and Wada, H. (1983) in *Methods in Biogenic Amine Research* (Parvez, S., Nagatsu, T., Nagatsu, I., and Parvez, H., eds) pp. 690–720, Elsevier Science Publications B.V., Amsterdam
23. Yoshinaga, K., Nishikawa, S., Ogawa, M., Hayashi, S., Kunisada, T., Fujimoto, T., and Nishikawa S. (1991) *Development* **113,** 689–699
24. Tajima, Y., Sawada, K., Morimoto, T., and Nishimune, Y. (1994) *J. Reprod. Fertil.* **102,** 117–122
25. Allison, A. C., and Hartree, E. F. (1970) *J. Reprod. Fertil.* **21,** 501–515
26. Zaneveld, L. J. D., and De Jonge, C. J. (1991) in *A Comparative Overview of Mammalian Fertilization* (Dunbar, B. S., and O'Rand, M. G., ed) pp. 63–79 Plenum Press, New York
27. Watabe, A., Fukui, T., Ohmori, E., and Ichikawa, A. (1992) *Biochem. Pharmacol.* **43,** 587–593
28. Yamamoto, J., Yatsunami, K., Ohmori, E., Sugimoto, Y., Fukui, T., Katayama T., and Ichikawa, A. (1990) *FEBS Lett.* **276,** 214–218
29. Ohtsu, H., Tanaka, S., Terui, T., Hori, Y., Makabe-Kobayashi, Y., Pejler, G Tchougounova, E., Hellman, L., Gertsenstein, M., Hirasawa, N., Sakurai E., Buzas, E., Kovacs, P., Csaba, G., Kittel, A., Okada, M., Hara, M., Ma L., Numayama-Tsuruta, K., Ishigaki-Suzuki, S., Ohuchi, K., Ichikawa, A Falus, A., Watanabe, T., and Nagy, A. (2001) *FEBS Lett.* **502,** 53–56
30. Tanaka, S., Hamada, K., Yamada, N., Sugita, Y., Tonai, S., Hunyady, Palkovits, M., Falus, A., Watanabe, T., Okabe, S., Ohtsu, H., Ichikawa, and Nagy, A. (2002) *Gastroenterology* **122,** 145–155
31. Sandlow, J. I., Feng, H., and Sandra, A. (1997) *Urology* **49,** 494–500
32. Dartsch, C., Chen, D., and Persson, L. (1998) *Regul. Pept.* **77,** 33–41
33. Fleming, J. V., and Wang, T. C. (2000) *Mol. Cell. Biol.* **20,** 4932–4947
34. Engel, N., Olno, M. T., Coleman, C. S., Medina, M. A., Pegg, A. E., Sánchez-Jiménez, F. (1996) *Biochem. J.* **320,** 365–368

Stimulation of bone formation and prevention of bone loss by prostaglandin E EP4 receptor activation

Keiji Yoshida*†‡, Hiroji Oida‡§, Takuya Kobayashi*, Takayuki Maruyama§, Masaharu Tanaka¶, Teruaki Katayama¶, Kojiro Yamaguchi¶, Eri Segi*, Tadao Tsuboyama†, Mutsumi Matsushita†, Kosei Ito‖, Yoshiaki Ito‖, Yukihiko Sugimoto**, Fumitaka Ushikubi††, Shuichi Ohuchida§, Kigen Kondo§, Takashi Nakamura†, and Shuh Narumiya*‡‡

Departments of *Pharmacology and †Orthopedic Surgery, Faculty of Medicine, **Department of Physiological Chemistry, Faculty of Pharmaceutical Sciences, and ‖Department of Viral Oncology, Institute for Virus Research, Kyoto University, Kyoto 606-8501, Japan; §Minase Research Institute and ¶Fukui Safety Research Institute, Ono Pharmaceutical Company, Osaka 618-8585, Japan; and ††Department of Pharmacology, Asahikawa Medical College, Asahikawa 078-8307, Japan

Communicated by John Vane, William Harvey Foundation, London, United Kingdom, January 19, 2002 (received for review October 30, 2001)

Bone remodeling, comprising resorption of existing bone and *de novo* bone formation, is required for the maintenance of a constant bone mass. Prostaglandin (PG)E_2 promotes both bone resorption and bone formation. By infusing PGE_2 to mice lacking each of four PGE receptor (EP) subtypes, we have identified EP4 as the receptor that mediates bone formation in response to this agent. Consistently, bone formation was induced in wild-type mice by infusion of an EP4-selective agonist and not agonists specific for other EP subtypes. In culture of bone marrow cells from wild-type mice, PGE_2 induced expression of core-binding factor α1 (Runx2/Cbfa1) and enhanced formation of mineralized nodules, both of which were absent in the culture of cells from EP4-deficient mice. Furthermore, administration of the EP4 agonist restored bone mass and strength normally lost in rats subjected to ovariectomy or immobilization. Histomorphometric analysis revealed that the EP4 agonist induced significant increases in the volume of cancellous bone, osteoid formation, and the number of osteoblasts in the affected bone of immobilized rats, indicating that activation of EP4 induces *de novo* bone formation. In addition, osteoclasts were found on the increased bone surface at a density comparable to that found in the bone of control animals. These results suggest that activation of EP4 induces bone remodeling *in vivo* and that EP4-selective drugs may be beneficial in humans with osteoporosis.

Bones undergo continuous remodeling through repeated cycles of destruction and rebuilding (1). This remodeling is mediated by the well balanced actions of osteoclasts, which resorb old bones, and osteoblasts, which form new bones. However, in the elderly, especially in postmenopausal women, the extent of bone resorption far exceeds that of bone rebuilding, resulting in osteoporosis and the associated increases in bone fragility and susceptibility to fractures (2). About 100 million people are estimated to suffer from this debilitating disease worldwide. Several drugs have been developed to treat osteoporosis, with most inhibiting bone resorption and only a few promoting bone formation (3). Such modulation of only one of the two processes in bone remodeling renders these drugs of limited efficacy in restoring the normal balance and bone mass.

Recently, significant advances have been made in our understanding of molecular mechanisms of osteoclast and osteoblast differentiation (4), but such knowledge has not been exploited fully to develop a drug that corrects the imbalance and restores normal bone remodeling. Prostaglandins (PGs) are a group of lipid mediators that are produced from arachidonic acid in a variety of tissues under various physiological and pathophysiological conditions and serve to maintain local homeostasis (5). Among them, PGs of the E type work bimodally in bone metabolism (6). PGE_2 potently induces bone resorption in bone organ cultures, whereas repeated injection of this compound *in vivo* induces bone formation in a variety of animals including humans. However, the use of PGE_2 as a therapeutic agent in the treatment of bone loss has been hindered by unwanted actions that systemically applied PGE_2 exerts in the body. It is not understood, either, the mechanism by which it induces bone formation or how this *in vivo* effect is related to its bone resorbing activity *in vitro*.

PGE_2 exerts its effects through interaction with specific cell surface receptors (5). Four subtypes of PGE receptors—EP1, EP2, EP3, and EP4—have been identified. These receptors are encoded by distinct genes and are expressed differentially in the body. With the use of homologous recombination, we have generated mice that lack each of the four EP subtypes individually (7–9). We also have screened compounds on a panel of the cloned receptors and developed drugs that act specifically at each EP subtype (10). With these tools, we now have investigated which EP subtype mediates the bone-forming activity of PGE_2 and how activation of this receptor induces bone formation. We have also used ovariectomized or immobilized rats as models of diseases with bone loss and examined the efficacy of EP-subtype-specific drugs in the treatment of this condition.

Materials and Methods

Mice. Mice deficient in each EP subtype (7–9) were backcrossed for more than five generations into C57BL/6CrSlc (Japan SLC, Hamamatsu, Japan). Males of the F2 progenies of N10 $EP1^{-/-}$ mice, N5 $EP2^{-/-}$ mice, and N5 $EP3^{-/-}$ mice were used. Because $EP4^{-/-}$ mice do not survive in the C57BL/6 background because of patent ductus arteriosus (8), survivors of F2 progenies in the mixed genetic background of 129/Ola × C57BL/6 were intercrossed and the resulting male survivors were used. Mice were treated according to the guidelines for the protection of experimental animals of Kyoto University and Ono Pharmaceutical.

Chemicals. DI-004, AE1–259, AE-248, and AE1–329, agonists for EP1, EP2, EP3, and EP4, respectively, were described (10). A new EP4 agonist, ONO-4819, methyl 7-[(1*R*, 2*R*, 3*R*)-3-hydroxy-2-[(*E*)-(3*S*)-3-hydroxy-4-(*m*-methoxymethylphenyl)-1-butenyl]-5-oxocyclopentyl]-5-thiaheptanoate (Patent Cooperation Treaty publish no. WO 00/03980), shows inhibition constant values of

Abbreviations: PG, prostaglandin; EP, PGE receptor; Cbfa1, core-binding factor α1; OVX, ovariectomized.

‡K.Y. and H.O. contributed equally to this work.

‡‡To whom reprint requests should be addressed at: Department of Pharmacology, Kyoto University Faculty of Medicine, Yoshida, Sakyo-ku, Kyoto 606-8501, Japan. E-mail: snaru@mfour.med.kyoto-u.ac.jp.

The publication costs of this article were defrayed in part by page charge payment. This article must therefore be hereby marked "*advertisement*" in accordance with 18 U.S.C §1734 solely to indicate this fact.

www.pnas.org/cgi/doi/10.1073/pnas.06205339

Table 1. Histomorphometric parameters in the tibia of sham-operated rats and immobilized rats with or without ONO-4819 treatment

Parameter*	Sham-operated rats (n = 4)	Control immobilized rats (n = 6)	ONO-4819-treated immobilized rats (n = 5)
Bone volume (BV/TV), %	7.82 ± 0.50	1.04 ± 0.38	13.4 ± 2.51†
Bone formation rate (BFR/TV), %/year	120.02 ± 7.77	17.01 ± 7.78	187.21 ± 42.97†
Bone surface (BS/TV), $\mu m/\mu m^2 \times 10^3$	3.49 ± 0.26	0.60 ± 0.19	6.37 ± 0.81†
Osteoid volume (OV/TV), %	0.39 ± 0.08	0.05 ± 0.02	1.17 ± 0.30†
Osteoid surface (OS/BS), %	30.39 ± 5.44	22.45 ± 5.18	44.51 ± 5.22†
Mineralizing surface (MS/OS), %	138.86 ± 19.68	78.41 ± 21.52	64.03 ± 11.01
Osteoblast surface (Ob.S/BS), %	11.90 ± 3.28	9.29 ± 3.01	22.38 ± 4.43†
Osteoclast surface (Oc.S/BS), %	13.81 ± 0.94	19.87 ± 4.40	15.09 ± 2.93
Osteoclast number (N.Oc/BS), no./mm	2.35 ± 0.33	3.22 ± 0.86	2.11 ± 0.48
Mineral apposition rate (MAR), μm/day	2.46 ± 0.11	2.20 ± 0.75	2.86 ± 0.12
Mineralization lag time (Mlt), day	1.14 ± 0.18	0.71 ± 0.23	2.48 ± 0.50†

*Nomenclature and abbreviations are from ref. 16.
†, $P < 0.05$ vs. immobilized control rats.

0.7, 56, and 620 nM for radioligand binding to EP4, EP3, and EP2, respectively, and values of more than 10 μM for EP1 and receptors for PGD_2, $PGF_2\alpha$, PGI_2, or thromboxane A_2. This compound was administered as an inclusion complex with α-cyclodextrin.

Local Infusion of PGE_2 and EP Agonists. Eight-week-old mice with body weights of 22–25 g were anesthetized. Their right femora were exposed, and the periosteum was removed around their shaft 8 mm in length. A polyvinyl catheter was fixed distally to the exposed bone surface and was connected proximally to an Alzet 1002 miniosmotic pump (Alza) implanted s.c. in the back and containing PGE_2 or EP agonists in ethanol/propylene glycol (40:60, vol/vol). The infusion was performed at a rate of 0.25 μl/hr for 6 weeks, with reservoir replacement every other week. The mice then were killed. Soft x-rays of the femur were taken as described (11). The anteroposterior and lateral diameters of the femur were measured in a callus-containing region of the treated bone and in the corresponding region of the contralateral femur. Each bone volume was calculated assuming the horizontal section of the femur to be elliptical, and the volume of the callus was obtained by subtraction. Histology of the femur was analyzed as described (12).

Bone Marrow Cell Culture. Bone marrow cells were obtained from femora of 8-week-old mice and cultured in the medium containing PGE_2 or vehicle as described (13). The medium was replaced every 3 days. After 21 days, the cells were rinsed with PBS, fixed in a 1:1:1.5 solution of 10% formalin/methanol/water for 2 h, and stained with the von Kossa method for mineralization. Nuclei were counterstained with neutral red. Photographs were taken with transmitted light, and the black-stained area of the mineralized nodules was measured with NIH IMAGE.

Immunoblot was performed as described with 100 μg protein of cell lysates and antibodies to core-binding factor α1 (Cbfa1) (14). Bound antibodies were detected with ECL Plus reagents (Amersham Pharmacia). Northern blot analysis was performed with 0.6 μg of poly(A) RNA. Hybridization was performed with random-primed ^{32}P-labeled probes prepared, with the 0.8-kb Eco*RI*-Hind*III* fragment of mouse Cbfa1 cDNA as a template (15).

Administration of ONO-4819 to Ovariectomized Rats. Fifteen-week-old female Crj:CD(SD)IGS (IGS) rats were anesthetized, and both ovaries were removed. ONO-4819 was dissolved in saline and administered either by i.v. infusion through a catheter into the right jugular vein or by s.c. injection in the back. Infusion was performed at a rate of 4 ml/kg per hr for 2 h twice per day. Seventy days after surgery, rats were killed and both femora and the fourth lumbar body were isolated. The right femur was fixed in 10% formalin and subjected to analysis with Micro Focus X-ray-Computed Tomography (MCT-CB100MF; Hitachi, Tokyo). The density of cancellous bone was measured in the left femur in a 0.77-mm-thick slice at a distance of 3 mm from the epiphysial growth plate by peripheral quantitative-computed tomography (Stratec Medizintechnik, Pforzeim, Germany) with a voxel size of 0.12 mm at a tube voltage of 50 kV. The lumbar body was used for compression testing, which was performed with a bone compression machine (MZ-500D; Maruto, Tokyo).

Immobilized Rat Model and Histomorphometric Analysis of Bone Tissues. Five- to six-week-old male IGS rats were anesthetized, and the left sciatic and femoral nerves each were resected at a length of 10 mm. Sham-operated rats received a similar operation without nerve resection. The rats then were systematically infused i.v. either with vehicle or ONO-4819 for 2 h twice a day. For bone density measurement, the rats were killed after 14 days, and the density of trabeculae of the left tibia was examined 4 mm from the proximal end as described above. For histomorphometric analysis, the infusion of ONO-4819 at 100 ng/kg per min or vehicle for 2 h twice a day continued for 28 days. On days 24 and 27, the rats received injection with tetracycline and calcein, respectively. After sacrifice on day 29, the left tibia was isolated. The sagittal block of the metaphysis was obtained, incubated with the Villanueva bone stain for 7 days, dehydrated, and embedded in methylmethacrylate. Sections of 4-μm thickness were prepared and subjected to the analysis by using a microscope coupled to the computerized bone morphometry analysis system (Luzex F Bone system, NIRECO, Tokyo). The primary parameters were measured as recommended (16) in an area between 1 and 1.2 mm from the growth plate and 200 μm apart from the cortical bone and were used to calculate the secondary parameters shown in Table 1.

Statistical Analysis. Data are presented as mean ± SE and were analyzed by using either Student's t test or, after variation analysis, Welch's t test or the Dunnett multiple comparison test. An associated probability (P value) of <0.05 was considered significant.

Results

Lack of PGE_2-Induced Bone Formation in $EP4^{-/-}$ Mice. By using a miniosmotic pump, we continuously infused PGE_2 into the periosteal region of the femur of wild-type C57BL/6 mice or

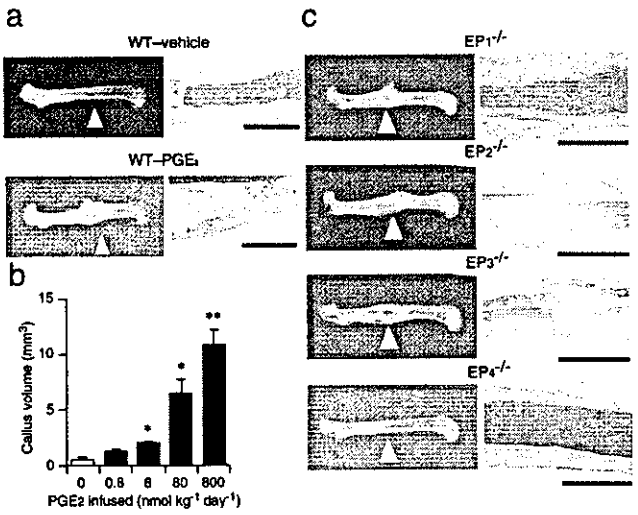

Fig. 1. Absence of PGE_2-induced bone formation in $EP4^{-/-}$ mice. (*a*) PGE_2-induced bone formation in wild-type mice. Typical radiographs (*Left*; arrowheads indicate the site of infusion) and histological preparations (*Right*; bars = 1 mm) of eight mice injected with vehicle or with PGE_2 at a dose of 800 nmol/kg per day are shown. (*b*) The dose dependence of the effect of PGE_2 on callus formation in wild-type mice. Data are values from six mice per dose. *, $P < 0.01$; **, $P < 0.001$ vs. vehicle-treated control mice. (*c*) The effect of PGE_2 on bone formation in EP-deficient mice. Typical radiographs (*Left*) and hematoxylin/eosin staining (*Right*) of the treated femur from each mouse strain infused with PGE_2 at a dose of 800 nmol/kg per day for 6 weeks are shown. Six mice per each strain were used in the analysis with reproducible results. (Bars = 1 mm.)

mice deficient in each EP subtype. After 6 weeks, the femur was isolated and bone formation was examined by both radiographic and histological analyses. Radiography revealed that PGE_2 induced extensive callus formation on the femur at the site of infusion in wild-type mice (Fig. 1*a*). The extent of callus formation depended on the dose of PGE_2 between 0.8 and 800 nmol/kg per day (Fig. 1*b*). Histological analysis showed marked thickening of the femoral cortex, with a large amount of woven bone as well as substantial accumulation of cells and bone matrix (Fig. 1*a*). Little bone formation was evident in the wild-type mice infused with vehicle alone. When PGE_2 was infused to mice deficient in each EP receptor subtype, the callus formation of as much extent as that seen in wild-type mice was observed in the cortex of the femora of $EP1^{-/-}$, $EP2^{-/-}$, and $EP3^{-/-}$ mice (Fig. 1*c*). This effect again depended on the doses of PGE_2 (data not shown). In contrast, no callus formation was detected in $EP4^{-/-}$ mice. On histology, massive formation of woven bone, similar to that apparent in wild-type animals infused with PGE_2, was seen in PGE_2-treated $EP1^{-/-}$, $EP2^{-/-}$, or $EP3^{-/-}$ mice but not in $EP4^{-/-}$ mice.

PGE_2 Induces Osteoblast Differentiation *in Vitro* Through EP4 Receptor Activation. The bone-forming activity of PGE_2 can be evaluated *in vitro* in a primary culture of rat bone marrow cells by measuring the formation of mineralized nodules (13). By application of this system to mice, we examined the mechanism of EP4-induced bone formation. Bone marrow cells were harvested from either wild-type C57BL/6 mice or $EP4^{-/-}$ mice and were cultured with PGE_2 for 3 weeks. Mineralized nodules were stained black by the von Kossa method, and their areas were summed. Culture of wild-type cells with vehicle alone resulted in the formation of mineralized nodules, and this was enhanced by the addition of PGE_2 in a concentration-dependent manner (Fig. 2*a*). In contrast, neither the basal level of mineralization nor its enhancement by PGE_2 was detected in cell culture derived from

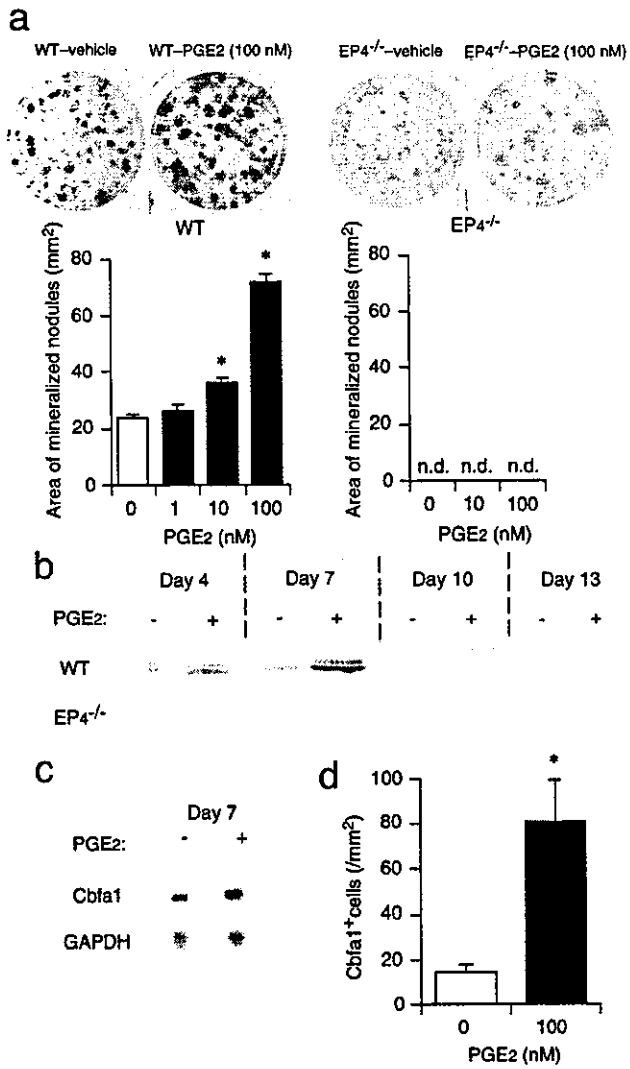

Fig. 2. EP4 mediates mineralized nodule formation and Cbfa1 expression in cultured bone marrow cells. (*a*) EP4-mediated enhancement of mineralized nodule formation by PGE_2. (*Upper*) von Kossa staining of mineralized nodules in bone marrow cell culture from wild-type C57BL/6 (WT) and $EP4^{-/-}$ mice in the presence of either vehicle or 100 nM PGE_2. Nuclei were counterstained with neutral red in the $EP4^{-/-}$ cell cultures. Typical results of six independent cultures are shown. (*Lower*) The concentration dependence of the effect of PGE_2 on mineralized nodule formation. Data are values from six experiments. *, $P < 0.001$ vs. vehicle-treated control. n.d., not detected. (*b*) Immunoblot analysis for Cbfa1 expression in bone marrow cells. Results of wild-type (WT) and $EP4^{-/-}$ cells cultured for indicated days in the absence or presence of 100 nM PGE_2 are shown. (*c*) Northern blot analysis for Cbfa1 mRNA abundance. Wild-type bone marrow cells cultured in the absence or presence of 100 nM PGE_2 for 7 days were subjected to Northern blot with probes specific to Cbfa1 or glyceraldehyde-3-phosphate dehydrogenase (GAPDH) mRNAs. (*d*) Effect of PGE_2 on the number of Cbfa1-positive cells. Bone marrow cells from wild-type mice cultured for 4 days in the absence or presence of 100 nM PGE_2 were stained with anti-mouse Cbfa1 antibody and visualized by the ABC method. The number of positive cells per culture was determined ($n = 10$). *, $P < 0.001$ vs. vehicle-treated culture.

$EP4^{-/-}$ mice. These results suggested that PGE_2 might promote osteoblast differentiation from precursor bone marrow cells. To test this possibility, we examined the effect of PGE_2 on the expression of Cbfa1 in these cells. Cbfa1 is an osteoblast-specific transcription factor and an important determinant of osteoblast differentiation (4, 17). Immunoblot analysis with mouse mAb

αA8G5 to Cbfa1 (14) detected two bands of ≈65 kDa in lysates prepared from vehicle-treated, wild-type cells on day 4 or 7 (Fig. 2*b*). The amounts of these proteins were markedly increased, and the duration of their expression was prolonged in cells cultured with 100 nM PGE_2. In contrast, only a very little amount of Cbfa1 was detected in vehicle-treated $EP4^{-/-}$ cells, and the abundance was not enhanced by the addition of PGE_2. These results suggest that PGE_2 increases the amount of Cbfa1 via EP4. This effect of PGE_2 appears to be exerted at the mRNA level, given that Northern blot analysis revealed that culture of wild-type cells with PGE_2 increased the level of Cbfa1 mRNA (Fig. 2*c*). Immunostaining of wild-type cultures with anti-Cbfa1 antibody revealed that incubation with PGE_2 induced a significant increase in the number of cells containing Cbfa1 immunoreactivity (Fig. 2*d*), indicating that PGE_2 increased the number of Cbfa1-expressing cells and not simply increased the amount of Cbfa1 in a fixed number of cells. These results taken together identify EP4 as the EP receptor subtype that mediates the bone-forming activity of PGE_2, and suggest that EP4 achieves this effect through induction of osteoblast differentiation.

An EP4-Selective Agonist Potently Stimulates Bone Formation *in Vivo*. To corroborate these observations pharmacologically, we next applied agonists DI-004, AE1–259, AE-248, and AE1–329, which specifically target EP1, EP2, EP3, and EP4, respectively (10). Wild-type mice were infused continuously with one of these compounds for 6 weeks, and their *in vivo* bone-forming activities were assessed. Infusion of the selective EP4 agonist, AE1–329, markedly increased bone formation, as detected both radiographically and histologically, in a dose-dependent manner (Fig. 3 *a* and *b*). In contrast, the femora of mice infused with each of the agonists specific for the other three EP subtypes did not appear to differ from those of animals infused with vehicle (Fig. 3 *c–e*). We also tested the *in vitro* activities of these agonists on the formation of mineralized nodules in primary cultures of bone marrow cells. AE1–329 again was the only one of four compounds capable of inducing mineralized nodule formation (data not shown).

Administration of an EP4 Agonist Prevents Bone Loss and Restores Bone Mass and Strength in Rats Subjected to Ovariectomy and Immobilization. Given that the EP4 agonist is a potent inducer of bone formation in healthy animals, we next investigated whether this type of drugs might exert a similar action in animals with bone loss and, thereby, restore bone mass and strength. To this end, we modified AE1–329 to increase its chemical stability (Fig. 4*a*). The resulting compound, ONO-4819, was administered to ovariectomized (OVX) rats, a model for human postmenopausal osteoporosis. Both ovaries were removed from 15-week-old female rats, and the effect of daily administration of ONO-4819 was examined. Seventy days after ovariectomy, vehicle-treated control OVX rats exhibited marked osteoporosis, as was apparent from the almost complete loss of bone trabeculae (Fig. 4*b*). s.c. injection of ONO-4819 three times per day beginning on the day of ovariectomy inhibited bone loss in a dose-dependent manner (Fig. 4 *b* and *c*); at a dose of 10 μg/kg, the drug completely prevented the bone loss. Importantly, the full restoration of bone density also was obtained when the injection was initiated 20 days after ovariectomy. We next evaluated the effect of the EP4 agonist on bone strength by subjecting the fourth lumbar body from these animals to the compression test. Ovariectomy resulted in a marked reduction in bone strength. This fragility was prevented by treatment of animals with ONO-4819 (Fig. 4*d*). In animals injected with ONO-4819 at 30 μg/kg three times per day or infused at 100 ng/kg per min for 2 h twice per day, bone strength was significantly greater than that in vehicle-treated OVX rats. Histology of bones revealed that trabeculae similar in architecture and appearance to those found in the sham-operated rats and lined with osteoblasts were formed in the OVX rats treated with ONO-4819 (Fig. 4*e*).

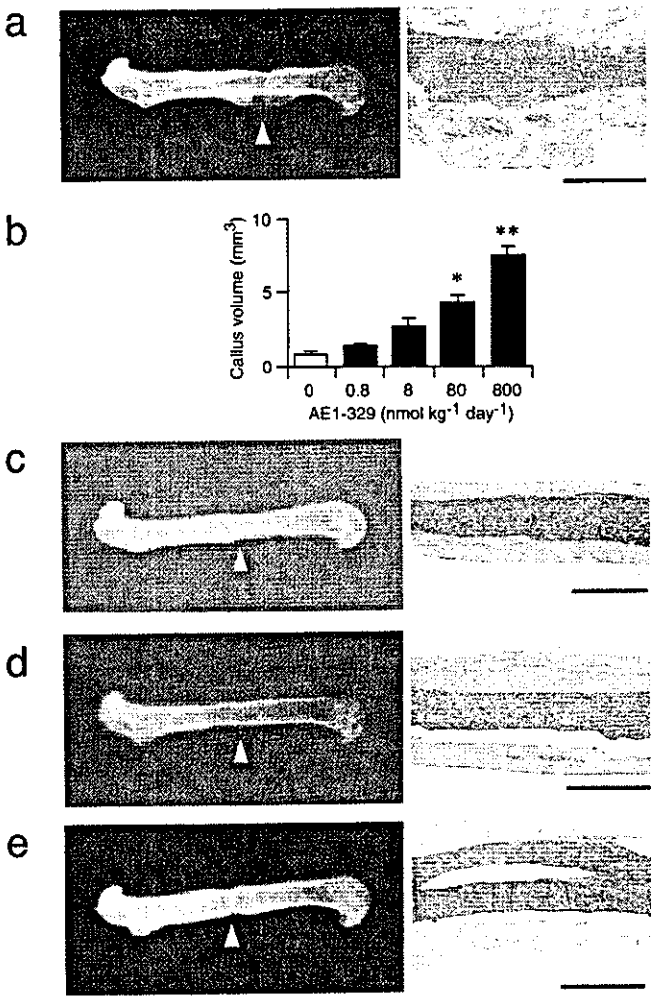

Fig. 3. Selective induction of bone formation by an EP4 agonist. Radiograph and histology of the femora treated with either the EP4 agonist AE1–329 (*a*), EP1 agonist DI-004 (*c*), EP2 agonist AE1–259 (*d*), or EP3 agonist AE-248 (*e*) are shown. Typical findings with a dose of 800 nmol/kg per day are shown. (Bars = 1 mm.) In *b*, the dose dependence of the effects of AE1–329 is shown. Data are from four animals per each dose. *, $P < 0.01$; **, $P < 0.001$ vs. vehicle-treated control.

In healthy animals, bone remodeling is stimulated by the mechanical tension applied to each bone as a result of its daily use, and prolonged immobilization results in a reduction in bone mass and deterioration of bone architecture. We therefore examined the effect of ONO-4819 on bone loss of immobilized rats. Immobilization of a hind limb induced a significant reduction in bone density of the tibia of the affected leg in 2 weeks. The infusion of ONO-4819 inhibited this reduction in a dose-dependent manner, preventing it completely at higher doses tested (Fig. 5). We next used rats subjected to this model and performed histomorphometric analysis on the effects of the ONO-4819 treatment (Table 1). Because the immobilization in our model affected significantly the cancellous bone and not the cortical bone, we limited our description to the changes in the cancellous bone of the metaphysis. This analysis revealed significant reduction in the volume of cancellous bone in immobilized rats as determined by bone volume (BV/TV). The ONO-4819 infusion significantly increased the bone volume including the osteoid volume and completely restored it in the immobilized

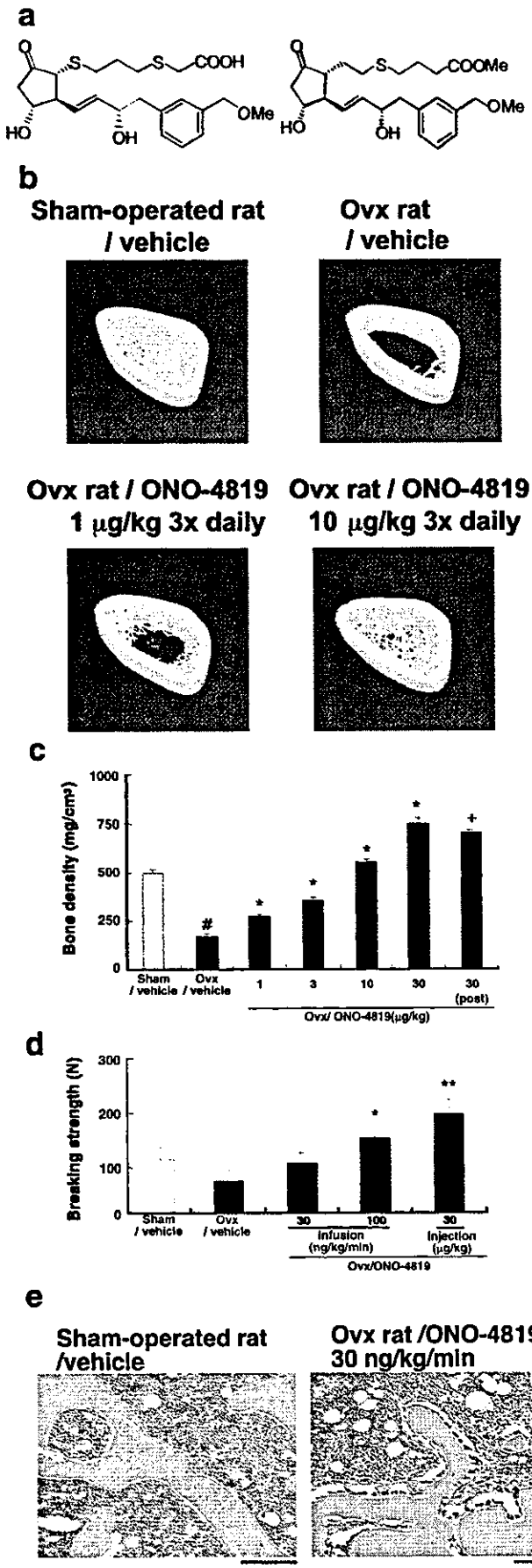

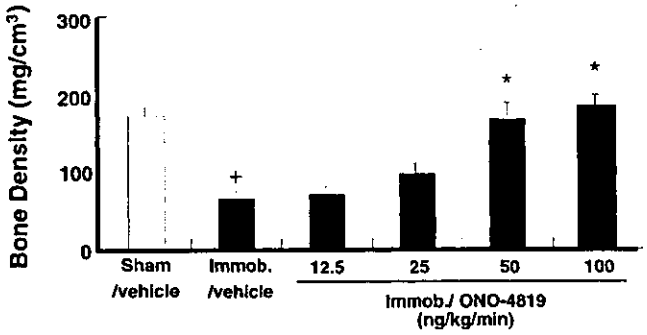

Fig. 5. Effects of ONO-4819 on immobilization-induced bone loss. Rats immobilized in the left hind limb (Immob) were infused systematically for 2 h twice per day with vehicle or the indicated doses of ONO-4819. After 14 days, the left tibia was isolated and subjected to analysis of bone density (n = 9–14 per group). +, $P < 0.01$ vs. the sham-operated group; *, $P < 0.01$ vs. control vehicle-treated immobilized group.

animals. This was reflected by the significant increase in bone formation rate in the ONO-4819-treated animals. The significant increases in bone surface (BS/TV) and in the bone surface lined with osteoblasts (Ob.S/BS) were also noted. These findings together with a similar density of osteoclasts on bone surface (N.Oc/BS) in ONO-4819-treated rats indicate that the total number of osteoclasts in the tissue markedly increased with the increase in the bone surface. On the other hand, the calcification rate as determined by double fluorescence labeling (mineral apposition rate) was not affected by this treatment.

In the above experiments, ONO-4819 administration caused no significant change in the serum concentrations of alkaline phosphatase, calcium, and inorganic phosphate in the animals (data not shown). Ectopic calcification in tissues such as cardiac valves or aorta was not found. No significant change in the blood pressure was detected in conscious rats by either infusion or injection of the drug at the doses described, although the infusion of the highest dose (100 ng/kg per min i.v.) induced less than 20% elevation of the heart rate.

Discussion

In this study, with both genetic and pharmacological approaches, we have unambiguously identified EP4 as the receptor that

Fig. 4. Prevention of bone loss and restoration of bone mass and strength by the EP4 agonist ONO-4819 in OVX rats. (*a*) Structure of AE1-329 (*Left*) and ONO-4819 (*Right*). (*b*) Bone architecture of OVX rats treated with ONO-4819. Seventy days after surgery, the right femur was isolated from a sham-operated rat as well as from OVX rats injected either with vehicle or two different doses of ONO-4819 and was subjected to analysis by x-ray-computed tomography. The three-dimensional structure was constructed by piling up images, and typical architecture of the metaphysis of each bone is presented. (*c*) Effects of ONO-4819 on bone density in OVX rats. OVX rats were injected s.c. with either vehicle or the indicated doses of ONO-4819 three times per day, either beginning on the day of surgery or day 20 after ovariectomy (post). Seventy days after the surgery, the left femur was isolated and subjected to analysis of bone density (n = 8 per group). #, $P < 0.05$ vs. the sham-operated group; *, $P < 0.05$ vs. control vehicle-treated OVX group (Dunnett test); +, $P < 0.05$ vs. control vehicle-treated OVX group (Student's t test). (*d*) Effects of ONO-4819 on bone strength in OVX rats. OVX rats were treated either by i.v. infusion of ONO-4819 at a rate of 30 or 100 ng/kg per min (≈15 and 50 nmol/kg per day) or by s.c. injection of the drug at a dose of 30 μg/kg three times per day (≈200 nmol/kg per day). Seventy days after surgery, rats were killed, and the fourth lumbar body was isolated and subjected to a compression test. No significant difference in the size of the bone was detected among the groups. Data are from eight rats per group. *, $P < 0.05$ vs. control vehicle-treated OVX group; *, $P < 0.01$ vs. control vehicle-treated OVX group. (*e*) Histology of the bone. Hematoxylin/eosin staining of the decalcified transverse sections of the epiphysis of the femur of sham-operated rats or OVX rats with ONO-4819 infusion is shown. (Bars = 100 μm.)

mediates the bone-forming activity of PGE_2. The role of this receptor in bone formation was suggested previously only indirectly by the use of a limited repertory of EP-acting compounds (18). We have found that activation of EP4 induced callus formation on the femur of mice and restored the volume of cancellous bone in OVX or immobilized rats. The histomorphometric analysis in the latter model revealed increases in both the total volume of the bone and the volume of osteoid, suggesting that these effects of the EP4 activation are exerted by *de novo* bone formation. *In vitro* in the bone marrow cell culture, EP4 activation increased the number of Cbfa-1-positive cells, suggesting that EP4 exerts such an effect by inducing osteoblast differentiation. Consistently, the density of osteoblasts lining the bone surface (Ob.S/BS) increased with ONO-4819 treatment in the *in vivo* models. It is noteworthy that the callus induced by PGE2 in mice contained many fibrous tissues and that the bone of ONO-4819-treated rats showed a mineralizing surface (MS/OS) of about half of that seen in sham-operated animals. These results indicate that the osteoblasts induced by EP4 activation produce bone matrix at a rate exceeding that of calcification. This was reflected by the prolonged mineralization lag time (Mlt) with an unchanged mineral apposition rate. However, the trabeculae formed were well connected, and the majority was sufficiently calcified as shown in Fig. 4*e* and Table 1, yielding substantial strength to the bone of OVX animals (Fig. 4*d*).

Our current study thus suggests that EP4 activation induces osteoblasts and thereby stimulates *de novo* bone formation. Previously, we also noted in bone organ culture that EP4 in mature osteoblasts mediates PGE_2-induced osteoclast differentiation (19, 20). We wondered how these two EP4 actions are coordinated *in vivo* in the bone of animals treated with the EP4 agonist. The bone morphometric analysis has shown that the EP4 agonist did not decrease the density of osteoclasts despite the increase in the bone surface, suggesting that it increased the number of osteoclasts in parallel with the *de novo* increase in bone. It is tempting to speculate that the PGE_2-EP4 signaling first works in osteoblast precursors to induce osteoblasts for bone formation and then works in mature osteoblasts for induction of osteoclasts on newly formed bones. Both EP4 and EP2 respond to PGE_2 and are coupled to activation of adenylate cyclase. Both also are implicated in PGE_2-induced osteoclastogenesis (19–21). It is interesting in this respect that we have not observed any involvement of EP2 in PGE_2-induced bone formation in mice (Figs. 1 and 3). We neither have observed any bone-forming effects of the EP2-selective agonist in OVX rats (data not shown). Although we cannot exclude a redundant role of EP2 in other species, these results indicate that EP4 is the only system mediating PGE_2-induced bone formation at least in rodents. It is curious, therefore, that the skeleton of $EP4^{-/-}$ mice either alive to adulthood or dead in the neonatal period is apparently normal (19, 20), suggesting that some pathway(s) other than the PGE_2 system works for physiological maintenance of bone. It remains to be clarified in what physiological or pathological context the PGE_2-EP4 signaling is mobilized for bone formation.

Several types of drugs currently are used for the treatment of bone loss (3). These drugs either inhibit differentiation and functions of osteoclasts or activate osteoblasts. However, none of these drugs are able to restore the balance between bone formation by osteoblasts and bone resorption by osteoclasts. PGE_2-EP4 appears to induce both osteoblastogenesis and osteoclastogenesis and to integrate the two actions temporarily and spatially *in situ* in bone remodeling. In this respect, the action of PGE_2 may be similar to that of PTH, which also promotes both bone formation and resorption (1, 3, 22). Recently, clinical efficacy of PTH for postmenopausal osteoporosis has been reported (23). On the other hand, the numerous, unwanted effects of PGE_2 injected systematically have precluded its use in therapeutics for bone loss. Because EP4 agonists are selective to only one subtype of EP receptors, they are expected to avoid several adverse actions caused by systemic administration of PGE_2. Indeed, ONO-4819 lacks the uterine-contracting activity of PGE_2. Furthermore, administration of ONO-4819 in rodents does induce diarrhea, hypotension, and thickening of intestinal epithelium but at higher doses than that required for bone formation. However, given various differences between the rodent models and human patients, it may be too early to conclude that EP4 agonists exert beneficial effects in humans. Their therapeutic potential will be tested rigorously in future studies.

We thank T. Komori for Cbfa1 cDNA, K. Deguchi for animal care and breeding, and T. Arai and H. Nose for secretarial assistance. This work was supported in part by Grants-in-Aid for Scientific Research from the Ministry of Education, Science, Sports and Culture of Japan and a grant from the Organization for Pharmaceutical Safety and Research.

1. Manolagas, S. C. (2000) *Endocr. Rev.* **21,** 115–137.
2. NIH Consensus Development Panel on Osteoporosis Prevention, Diagnosis and Therapy (2001) *J. Am. Med. Assoc.* **285,** 785–795.
3. Rodan, G. A & Martin, T. J. (2000) *Science* **289,** 1508–1514.
4. Karsenty, G. (1999) *Genes Dev.* **13,** 3037–3051.
5. Narumiya, S., Sugimoto, Y. & Ushikubi, F. (1999) *Physiol. Rev.***79,** 1193–1226.
6. Pilbeam, C. C., Harrison, J. R. & Raisz, L. G. (1996) in *Principles of Bone Biology*, eds. Bilekizian, J. P., Raisz, L. G. & Rodan, G. A. (Academic, San Diego), pp. 715–728.
7. Ushikubi, F., Sugimoto, Y., Murata, T., Matsuoka, T., Kobayashi, T., Segi, E., Hizaki, K., Ichikawa, A., Tanaka, T., Yoshida, N., *et al.* (1998) *Nature (London)* **395,** 281–284.
8. Segi, E., Sugimoto, Y., Yamasaki, A., Aze, Y., Oida, H., Nishimura, T., Murata, T., Ushukubi, F., Fukumoto, M., Tanaka, T., *et al.* (1998) *Biochem. Biophys. Res. Commun.* **246,** 7–12.
9. Hizaki, H., Segi, E., Sugimoto, Y., Hirose, M., Saji, T., Ushikubi, F., Matsuoka, T., Noda, Y., Tanaka, T., Yoshida, N., *et al.* (1999) *Proc. Natl. Acad. Sci. USA* **96,** 10501–10506.
10. Suzawa, T., Miyaura, C., Inada, M., Maruyama, T., Sugimoto, Y., Ushikubi, F., Ichikawa, A., Narumiya, S. & Suda, T. (2000) *Endocrinology* **141,** 1554–1559.
11. Matsushita, M., Tsuboyama, T., Kasai, R., Okumura, H., Yamamuro, T., Higuchi, K., Higuchi, K., Kohno, A., Yonezu, T., Utani, A., *et al.* (1986) *Am. J. Pathol.* **125,** 276–283.
12. Okamoto, Y., Takahashi, K., Toriyama, K., Takeda, N., Kitagawa, K., Hosokawa, M. & Takeda, T. (1995) *Anat. Rec.* **242,** 21–28.
13. Weinreb, M., Suponitzky, I. & Keila, S. (1997) *Bone* **20,** 521–526.
14. Zhang, Y.-W., Yasui, N., Ito, K., Huang, G., Fujii, M., Hanai, J., Nogami, H., Ochi, T., Miyazono, K. & Ito, Y. (2000) *Proc. Natl. Acad. Sci. USA* **97,** 10549–10554.
15. Ogawa, E., Maruyama, M., Kagoshima, H., Inuzuka, M., Lu, J., Satake, M., Shigesada, K. & Ito, Y. (1993) *Proc. Natl. Acad. Sci. USA* **90,** 6859–6863.
16. Parfitt, A. M., Drezner, M. K., Glorieux, F. H., Kanis, J. A., Malluche, H., Meunier, P. J., Ott, S. M. & Recker, R. R. (1987) *J. Bone Miner. Res.* **2,** 595–610.
17. Komori, T., Yagi, H., Nomura, S., Yamaguchi, A., Sasaki, K., Deguchi, K., Shimizu, Y., Bronson, R. T., Gao, Y. H., *et al.* (1997) *Cell* **89,** 755–764.
18. Machwate, M., Harada, S., Leu, C. T., Seedor, G., Labelle, M., Gallant, M., Hutchins, S., Lachance, N., Sawyer, N., Slipetz, D., *et al.* (2001) *Mol. Pharmacol.* **60,** 36–41.
19. Sakuma, Y., Tanaka, K. Suda, M., Yasoda, A., Natsui, K., Tanaka, I., Ushikubi, F., Narumiya, S., Segi, E., Sugimoto, Y., *et al.* (2000) *J. Bone Miner. Res.* **15,** 218–227.
20. Miyaura, C., Inada, M., Suzawa, T., Sugimoto, Y., Ushikubi, F., Ichikawa, A., Narumiya, S. & Suda, T. (2000) *J. Biol. Chem.* **275,** 19819–19823.
21. Li, X., Okada, Y., Pilbeam, C. C., Lorenzo, J. A., Kennedy, C. R., Breyer, R. M. & Raisz, L. G. (2000) *Endocrinology* **141,** 2054–2061.
22. Dobnig, H. & Turner, R. T. (1997) *Endocrinology* **138,** 4607–4612.
23. Neer, R. M., Arnaud, C. D., Zanchetta, J. R., Prince, R., Gaich, G. A., Reginster, J.-Y., Hodsman, A. B., Eriksen, E. F., Ish-Shalom, S., Genant, H. K., *et al.* (2001) *N. Eng. J. Med.* **344,** 1434–1441.

Antigen-independent Induction of Histamine Synthesis by Immunoglobulin E in Mouse Bone Marrow–derived Mast Cells

Satoshi Tanaka, Yuhji Takasu, Sonoko Mikura, Norio Satoh, and Atsushi Ichikawa

Department of Physiological Chemistry, Graduate School of Pharmaceutical Sciences, Kyoto University, Sakyo-ku, Kyoto 606-8501, Japan

Abstract

Immunoglobulin (Ig)E-mediated activation of mast cells has long been thought to occur only when FcεRI receptor-bound IgE is cross-linked via multivalent antigens. However, recent studies have raised the possibility that mast cells may be activated by the binding of IgE to the FcεRI receptor in the absence of antigen. Here we demonstrate that IgE binding without antigen induces the expression of histidine decarboxylase (HDC) in mouse interleukin (IL)-3–dependent bone marrow–derived mast cells (BMMCs). The induction of HDC by the binding of IgE was found to require an influx of extracellular calcium ions, which was attenuated by pretreatment with U73122, a phospholipase C inhibitor. Furthermore, the increase in HDC activity upon sensitization with IgE was completely suppressed by pretreatment of BMMCs with protein kinase C inhibitors, such as H7, staurosporine, and Gö6976. In addition, immediate activation of the tyrosine kinase Lyn was not detectable upon treatment with IgE. These results suggest that the binding of IgE to its receptor in the absence of antigen results in de novo synthesis of HDC in BMMCs through a signaling pathway distinct to that operating during antigen-stimulated FcεRI activation.

Key words: histidine decarboxylase • enzyme induction • protein kinase C • calcium signaling • IgE receptors

Introduction

Mast cells are found in various tissues throughout the body and trigger allergic and inflammatory responses by releasing a wide variety of mediators, such as histamine, arachidonic acid metabolites, and neutral proteases (1, 2). Activation and signaling of FcεRI, the high-affinity receptor for IgE, has long been thought to occur only when receptor-bound IgE is cross-linked via multivalent antigens (1–4). However, recently reported evidence has raised the possibility that higher concentrations of IgE can trigger a number of signaling pathways in mast cells and circulating basophils, even in the absence of antigens. Treatment of cells with IgE in the absence of antigen was found to enhance the expression of FcεRI by various mast cell populations in vitro and in mouse peritoneal cells in vivo (5–8). It has been demonstrated that IL-3–dependent bone marrow–derived mast cells (BMMCs)* respond with an increase in cytosolic Ca^{2+} levels when treated with IgE alone (9) and that monomeric IgE stimulates multiple phosphorylation events in mouse BMMCs, leading to potent cytokine production and enhanced survival (10, 11). These observations suggest that monomeric IgE is involved in the activation of mast cells, which is distinct from induction via antigen stimulation.

The above studies have indicated that monomeric IgE in the absence of antigen may not be able to stimulate the degranulation and release of histamine from mast cells. However, the regulation of histamine synthesis by monomeric IgE remains to be clarified. We previously purified L-histidine decarboxylase (HDC), the rate-limiting enzyme of histamine synthesis in mammals, cloned its cDNA from a mouse mastocytoma cell line, and prepared a specific antibody for HDC, in order to elucidate the mechanism regulating histamine synthesis (12, 13). As previous reports have demonstrated that atopic patients, who possess extremely

Address correspondence to Atsushi Ichikawa, Department of Physiological Chemistry, Graduate School of Pharmaceutical Sciences, Kyoto University, Sakyo-ku, Kyoto 606-8501, Japan. Phone: 81-75-753-4527; Fax: 81-75-753-4557; E-mail: aichikaw@pharm.kyoto-u.ac.jp

**Abbreviations used in this paper:* BMMC, IL-3-dependent bone marrow–derived mast cell; HDC, L-histidine decarboxylase; MEK, MAPK/ERK kinase; PI3-kinase, phosphoinositide 3-kinase; PLC, phospholipase C; PKC, protein kinase C; TPA, 12-O-tetradecanoyl phorbol 13-acetate.

J. Exp. Med. © The Rockefeller University Press • 0022-1007/2002/07/229/7 $5.00
Volume 196, Number 2, July 15, 2002 229–235
http://www.jem.org/cgi/doi/10.1084/jem.20012037

high concentrations of serum IgE, show higher serum histamine concentrations than normal individuals (14, 15), we hypothesized that monomeric IgE may be involved in the up-regulation of HDC. The purpose of our present study was to investigate the effects of monomeric IgE on histamine synthesis and to identify the signaling pathway involved in this histamine synthesis.

Materials and Methods

Mice. Specific pathogen-free, 8-wk-old female Balb/c mice were obtained from Japan SLC.

Materials. The anti-HDC antibody was prepared as described previously (16). The following materials were commercially obtained from the sources indicated: an anti-DNP mouse monoclonal IgE (SPE-7) and DNP-conjugated human serum albumin from Sigma-Aldrich, an anti-DNP IgG (HDP-1) from Oxford Biomedical Research, an anti-trinitrophenyl IgE and an anti-mouse FcγRIIB/III (2.4G2) antibody from BD Biosciences, mouse whole IgG molecule from CHEMICON International Inc. [α-^{32}P]dCTP (3,000 Ci/mmol), and [γ-^{32}P]ATP (3,000 Ci/mmol) from Du Pont-New England Nuclear, a horseradish peroxidase–conjugated anti-rabbit IgG antibody from Dako, an ECL kit from Amersham Biosciences, Fura-2/AM from Dojindo Laboratories, an agarose-conjugated anti-Lyn antibody, and an anti-Lyn mouse monoclonal antibody from Santa Cruz Biotechnology, Inc. All other chemicals were commercial products of reagent grade.

Preparation of BMMCs. BMMCs were prepared as described previously with minor modifications (17). Cells were cultured in the complete RPMI containing 50% WEHI-3–conditioned medium as a source of IL-3 and 10% fetal bovine serum at 37°C in a fully humidified 5% CO_2 atmosphere. After 4 wk of culture, >95% of the viable cells were confirmed to be immature mast cells, as assessed by staining with acidic Toluidine blue. A linear increase in the surface expression of FcεRI was observed upon flow cytometric analyses in the presence of 3 μg/ml anti-DNP IgE (data not shown), which is consistent with previous studies (7, 8).

HDC Assay. Cells were rinsed with PBS followed by centrifugation and the cell pellet was lysed (10^7 cells/ml) with 10 mM HEPES–NaOH, pH 7.3, containing 1.5 mM $MgCl_2$, 10 mM KCl, 0.5 mM dithiothreitol, 1 mM EDTA, 1 mM EGTA, 1% Triton X-100, and a protease inhibitor mixture (0.2 mM PMSF, 10 μg/ml aprotinin, 10 μg/ml leupeptin, 0.1 mM benzamidine, 1 μg/ml pepstatin A, and 10 μg/ml E-64) on ice for 30 min. The cells were centrifuged at 100,000 *g* for 1 h at 4°C and the supernatant was used for the measurement of HDC activity as described previously (18).

Northern Blot Analyses. Total RNA was extracted from cells using ISOGEN (Nippon Gene), according to the manufacturer's instructions. Total RNA (3 μg) obtained was electrophoretically separated on a 1.5% agarose/formaldehyde gel. After electrophoresis, the RNA was transferred onto a Biodyne A membrane (Pall) in 20× SSC (1× SSC is composed of 0.15 M NaCl and 0.015 M sodium citrate) by capillary blotting. [^{32}P]-Labeled specific cDNA probes were synthesized in the presence of [α-^{32}P]dCTP and hybridized onto the filter in hybridizing solution (6× SSC, 5× Denhardt's solution, 0.5% SDS, and 100 μg/ml salmon sperm DNA) at 68°C overnight. The filter was rinsed twice in 2× SSC at room temperature and twice in 2× SSC containing 1% SDS at 60°C. The filter was then analyzed using a Fujix BAS 2000 Bio-Imaging Analyzer.

Immunoblot Analyses. Cells were homogenized in 50 mM HEPES–NaOH, pH 7.3, containing 1 mM dithiothreitol, 1% Triton X-100, and the protease inhibitor mixture, and centrifuged at 15,000 *g* for 30 min at 4°C. The resultant supernatant (50 μg protein/lane) was subjected to SDS-PAGE (10% slab gel), and the separated proteins were transferred electrophoretically onto a PVDF membrane (Millipore). Immunoblot analysis was performed as described previously (18). An anti-HDC antibody (1:500) was used as the primary antibody, and a horseradish peroxidase–conjugated anti–rabbit IgG antibody (1:3,000) was used as the secondary antibody. The membranes were stained using an ECL kit according to the manufacturer's instructions.

Cell Culture Under Ca^{2+}-free Conditions. Cells were washed twice in PIPES buffer (25 mM PIPES, pH 7.4, containing 125 mM NaCl, 2.7 mM KCl, 5.6 mM glucose, 1 mM $CaCl_2$, and 0.1% bovine serum albumin), or in Ca^{2+}-free PIPES buffer. The cells were then incubated in buffer with or without Ca^{2+} in the presence or absence of 3 μg/ml IgE for 90 min at 37°C. The cells were harvested and Northern blot analyses were performed as described above.

Measurement of Cytosolic Ca^{2+} Concentrations. Cells were loaded with 2 μM Fura-2/AM in modified Tyrode's buffer (130 mM NaCl containing 5 mM KCl, 1.4 mM $CaCl_2$, 1 mM $MgCl_2$, 5.6 mM glucose, 10 mM HEPES, NaOH, pH 7.3, and 0.1% bovine serum albumin) for 45 min at room temperature and then washed in modified Tyrode's buffer. For Ca^{2+} free conditions, the buffer was replaced with Ca^{2+} free modified Tyrode's buffer containing 0.3 mM EGTA. Fluorescent intensities were measured, at an excitation wavelength of 340 or 380 nm and an emission wavelength of 510 nm, with a fluorescence spectrometer (CAF-100; Jasco) as described previously (19).

Treatment with Various Kinase Inhibitors. BMMCs were treated for the indicated periods with various kinase inhibitors at the concentrations indicated, before the addition of IgE. Protein kinase C (PKC) inhibitors: Staurosporine (10 min, 1 μM), H7 (30 min, 0.1 mM), chelerythrine chloride (60 min, 10 μM), Gö6976 (60 min, 10 μM), PKC inhibitors 19–27, myristoylated peptide (60 min, 0.1 mM), Ro-32–0432 (60 min, 1 μM), and bisindolylmaleimide (25 min, 1 μM); tyrosine kinase inhibitors: herbimycin A (30 min, 1.5 μM), genistein (30 min, 0.1 mM), PP2 (10 min, 10 μM), and PP3, an inactive analogue of PP2 (10 min, 10 μM); other inhibitors: H89 (protein kinase a [PKA], 30 min, 10 μM), PD98059 (mitogen-activated protein kinase [MAPK]/ERK kinase [MEK], 30 min, 50 μM), SB203580 (p38, 30 min, 10 μM), LY294002 (phosphoinositide 3 [PI3]-kinase, 30 min, 50 μM), wortmannin (PI3-kinase, 15 min, 0.1 μM), and W7 (calmodulin, 30 min, 10 μM).

Immunoprecipitation and In Vitro Kinase Assay for Lyn. Cells were incubated in the presence or absence of 3 μg/ml anti-DNP IgE for 5 min. In the experiment of antigen stimulation, cells were incubated with 1 μg/ml anti-DNP IgE for 12 h and then stimulated by the addition of antigens (30, 100, and 300 ng/ml DNP-human serum albumin) for 5 min. Immunoprecipitation with an agarose-conjugated anti-Lyn antibody (20 μg/ml) was performed as described previously (18) in the presence of 1 mM sodium vanadate. The resultant precipitate was washed four times with the RIPA buffer followed by two times of washing with 20 mM HEPES-NaOH, pH 8.0, containing 150 mM NaCl, 10 mM magnesium acetate, and 20 mM $MnCl_2$ (kinase assay buffer). The precipitate was incubated in kinase assay buffer containing 10 μM ATP in the presence of 10 μCi [γ-^{32}P]ATP for 5 min at 30°C.

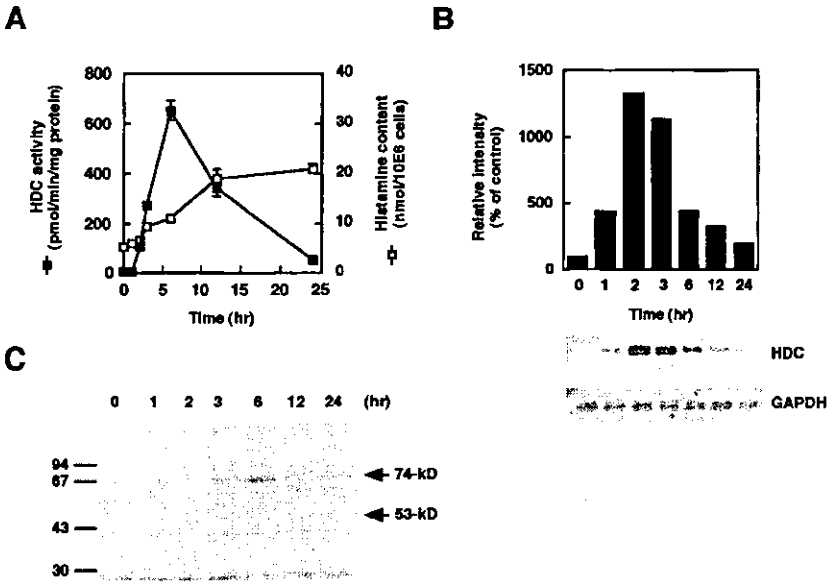

Figure 1. Time course of HDC activity and mRNA accumulation induced by IgE. BMMCs were cultured in the presence of 3 μg/ml anti-DNP IgE for the periods indicated. (A) HDC activity (closed boxes) and histamine content (open boxes) of the cells are demonstrated. The values are represented as the means ± SEM (n = 3). (B) Transient increase in HDC mRNA accumulation is represented. The relative intensities of the bands hybridized with the probe for HDC were normalized by those with the probe for glyceraldehyde-3-phosphate dehydrogenase (GAPDH). This is a representative figure of three independent experiments showing similar results. (C) The result of immunoblot analyses using an anti-HDC antibody is demonstrated. The arrows indicate the position of the 74-kD form (74-kD) and 53-kD form (53-kD) of HDC. Note that the 53-kD form is undetectable.

Immunoblot analyses were also performed as described above using an anti-Lyn mouse monoclonal antibody (1:200) to confirm an equal amount of precipitated Lyn.

Results

Induction of Histamine Synthesis by IgE in the Absence of Antigen. We found significant increases in the HDC activity of BMMCs upon sensitization with IgE. Among the various types of IgG and IgE, only anti-DNP IgE drastically induced HDC activity in BMMCs in the absence of antigen 6 h after stimulation (Table I). Both the anti-DNP IgG and the polyclonal IgG mixture were unable to increase the HDC activity of BMMCs. IgE has been shown to bind to the Fc receptors for IgG (FcγRII and FcγRIII), in addition to FcεRI in mouse BMMCs (20), and IgE-mediated systemic anaphylaxis has been shown to be enhanced in FcγRII-deficient mice whereas being attenuated in FcγRIII-deficient mice (21). Blockage of these FcγRs with the 2.4G2 antibody has no effect on the increase in HDC activity induced by IgE. The HDC activity of BMMCs increased dose dependently by anti-DNP IgE treatment, and plateau levels were reached at >3 μg/ml anti-DNP IgE (data not shown). Northern blot analyses revealed that this induction occurs in the transcriptional level and a >10-fold increase was observed by the addition of 3 μg/ml anti-DNP IgE (Fig. 1 B). This induction of HDC in BMMCs was found to be transient. A significant increase in the HDC activity was first observed 2 h after the addition of anti-DNP IgE, and a maximal level of HDC activity was obtained 6 h after the addition of anti-DNP IgE (Fig. 1 A). A significant increase in HDC mRNA expression was observed 1 h after stimulation with anti-DNP IgE (Fig. 1 B). Cellular histamine content significantly increased at a later phase (12 h) with an approximately fourfold increase in histamine content being detected 24 h after the addition of anti-DNP IgE (Fig. 1 A). Immunoblot analyses using an anti-HDC antibody revealed that the dominant form of HDC induced in the BMMCs was the 74-kD form (Fig. 1 C). The 53-kD form of HDC, which we previously reported to be found in a rat mast cell line (18), was hardly detectable in the BMMCs both in the presence and absence of anti-DNP IgE (Fig. 1 C).

Table I. *Increase in HDC Activity Induced by IgE or Various Activators of the Ca^{2+}–PKC Pathway*

	HDC activity
	pmol/min/mg protein
None	3.13 ± 1.68
Anti-DNP IgE	652 ± 54.8[a]
Anti-DNP IgG	5.80 ± 1.95
Polyclonal IgG	1.43 ± 1.00
Anti-DNP IgE + 2.4G2	626 ± 46.2[a]
IgE/antigen	389 ± 10.3[a, b]
Thapsigargin	618 ± 162[a]
TPA	96.3 ± 23.3[a]
A23187	1,240 ± 118[a]

BMMCs were cultured in the presence of an anti-DNP IgE (3 μg/ml), an anti-DNP IgG (3 μg/ml), purified polyclonal IgG (3 μg/ml), thapsigargin (100 nM), TPA (10 nM), and A23187 (0.3 μM) for 6 h at 37°C. Blocking of FcγRII and FcγRIII was performed by pretreatment with the 2.4G2 antibody (10 μg/ml) for 10 min. In the experiment of antigen stimulation (IgE/antigen), BMMCs were incubated in the presence of 1 μg/ml anti-DNP IgE for 24 h at 37°C, washed, and then incubated with 30 ng/ml DNP-human serum albumin for 6 h. The concentration of each reagent was optimized in preliminary experiments to obtain its maximal effect. The values obtained are represented as the means ± SEM (n = 3).
[a] $P < 0.01$ is regarded as significant by the Student's t test (vs. None).
[b] $P < 0.05$ is regarded as significant by the Student's t test (vs. Anti-DNP IgE).

Requirement of Extracellular Ca^{2+} Influx for the Induction of HDC mRNA. As monomeric IgE has been found to increase cytoplasmic Ca^{2+} levels in BMMCs (9), the effect of extracellular Ca^{2+} on the induction of HDC mRNA by anti-DNP IgE was investigated. Induction of HDC mRNA by anti-DNP IgE was completely suppressed by the depletion of extracellular Ca^{2+} (Fig. 2 A). The addition of anti-DNP IgE caused an increase in cytosolic Ca^{2+}, which was completely suppressed by pretreatment with a phospholipase *c* (PLC) inhibitor, U73122 (Fig. 2 B). The increase in cytosolic Ca^{2+} induced by anti-DNP IgE was sustained for a longer period compared with that induced by antigen stimulation. U73343, an inactive analogue of U73122, was unable to suppress the increase in cytosolic Ca^{2+} induced by both the addition of anti-DNP-IgE and antigen stimulation. A slight increase in cytoplasmic Ca^{2+} by anti-DNP IgE was also observed in the absence of extracellular Ca^{2+}, which was also attenuated by pretreatment with U73122 (Fig. 2 C).

Effects of 12-O-Tetradecanoyl Phorbol 13-Acetate, Thapsigargin, and A23187 on the Induction of HDC. The effects of various activators of the Ca^{2+}-PKC pathway on the induction of HDC activity were investigated. A phorbol ester, 12-O-tetradecanoyl phorbol 13-acetate (TPA), which is known to be an activator of PKC, slightly but significantly induced HDC activity in the BMMCs, whereas thapsigargin, an inhibitor of the Ca^{2+}-ATPase in the endoplasmic reticulum, and A23187, a calcium ionophore, drastically increased HDC activity in the BMMCs, to levels comparable to those induced by anti-DNP IgE (Table I). Cross-linking of the FcεRI with multivalent antigens also caused the induction of HDC, and this inducible effect was smaller than that induced by IgE alone (Table I). The accumulation of HDC mRNA in the cells activated by antigen stimulation was also observed but was smaller than that observed in cells treated with anti-DNP IgE alone (data not shown).

Effects of Various Kinase Inhibitors on HDC Expression Induced by IgE. The effects of an array of kinase inhibitors on the induction of HDC were investigated. PKC inhibitors, such as staurosporine, H7, and Gö6976, significantly suppressed the increase of HDC activity and mRNA expression whereas the other PKC inhibitors did not (Fig. 3, A and C). Chelerythrine moderately suppressed the increase in HDC activity but not the increase in mRNA expression. Inhibitors of PKA (H89), MEK (PD98059), p38 (SB203580), calmodulin (W7), and PI3-kinase (LY294002, and wortmannin) were all ineffective in suppressing the induction of HDC activity (Fig. 3, A and B). The Src family protein tyrosine kinase inhibitors, herbimycin A and PP2, had a modest inhibitory effect on the induction of HDC (Fig. 3, A and D). All the other inhibitors tested were ineffective in inhibiting the induction of HDC.

Absence of Lyn Activation. As the protein tyrosine kinase Lyn has been found to play critical roles in the early events induced by the cross-linking of the FcεRI (22), in vitro kinase assay for Lyn was performed in BMMCs. A significant increase in [^{32}P] incorporation was observed in the bands, of which molecular mass was 53 and 56 kD, concentration dependently by antigen stimulation, whereas no changes were seen upon treatment with anti-DNP IgE alone (Fig. 4). Immunoblot analyses using an anti-Lyn antibody indicated that each immunoprecipitate contained the same amounts of Lyn.

Discussion

We have demonstrated that IgE is able to induce histamine synthesis in mouse BMMCs even in the absence of antigen. Recent research has clearly demonstrated that monomeric IgE activates mouse BMMCs exclusively via their FcεRI (10, 11). We performed this study using the same commercial IgE preparation (SPE-7; Sigma-Aldrich) as these previous studies. Stimulation of FcγRII and FcγRIII by anti-DNP IgG or by polyclonal IgG caused no signifi-

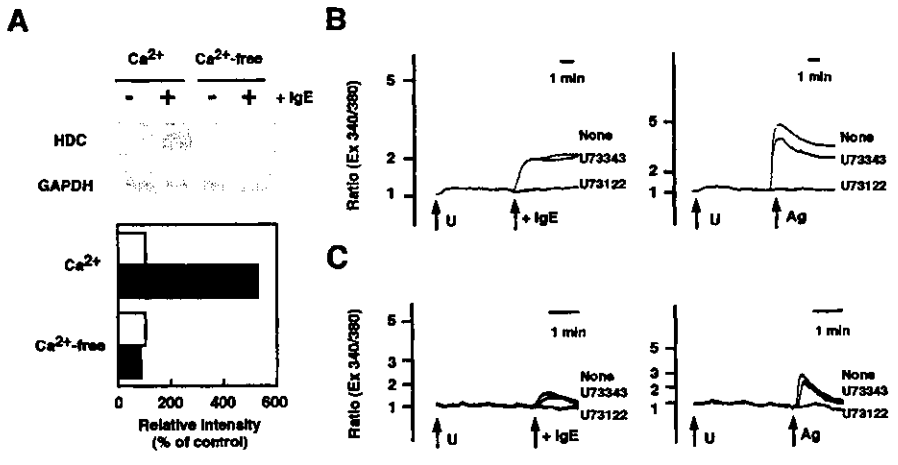

Figure 2. Requirement of extracellular Ca^{2+} for the induction of HDC by IgE. (A) BMMCs were incubated in PIPES buffer with (Ca^{2+}) or without Ca^{2+} (Ca^{2+}-free) for 90 min in the presence (black bars) or absence (white bars) of 3 μg/ml anti-DNP IgE. The cells were then harvested and Northern blot analyses were performed. The relative intensities of the hybridized bands are demonstrated as described in the legend to Fig. 1. This is a representative figure of three independent experiments showing similar results. (B and C) Ca^{2+} influx induced by anti-DNP IgE was compared with that induced by antigen stimulation. BMMCs were loaded with 2 μM Fura-2/AM in modified Tyrode's buffer in the presence (B) or absence (C) of Ca^{2+} as described in Materials and Methods. U73122 or U73343 (3 μM) was added (U) 3 min (C) or 7 min (B) before the stimulation. (Left panels) Stimulation with anti-DNP IgE (10 μg/ml) added to the culture. (Right panels) Stimulation with antigen (Ag, DNP-human serum albumin, 30 ng/ml) after 12 h of sensitization with anti-DNP IgE (1 μg/ml).

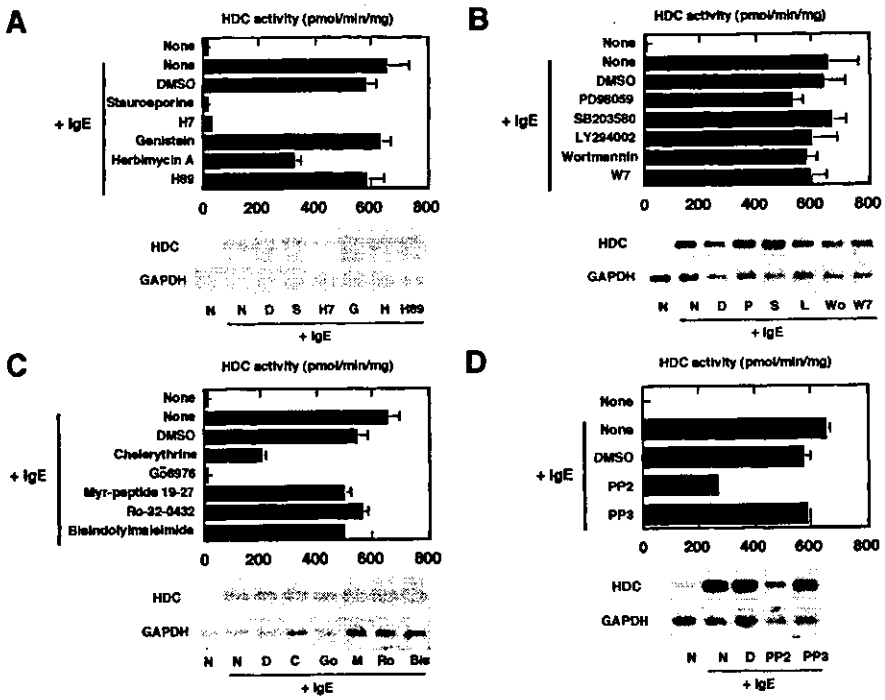

Figure 3. Effects of various kinase inhibitors on the induction of HDC by IgE. BMMCs were pretreated with various kinase inhibitors as described in Materials and Methods. The cells were further incubated in the presence or absence of 3 μg/ml anti-DNP IgE for 3 h (for Northern blot) or 6 h (for HDC activity). (Top panels) HDC activity of the cells is presented. The values are represented as the means ± SEM (n = 3). (Bottom panels) HDC mRNA accumulation in the cells were measured by Northern blot analyses. The relative intensities of the hybridized bands are demonstrated as described in the legend to Fig. 1. This is a representative figure of three independent experiments showing similar results.

cant changes in HDC activity. Furthermore, blocking of these FcγRs by the 2.4G2 antibody did not alter the activation of HDC by IgE, indicating that FcγRII and FcγRIII may not be involved in the induction of HDC. Intracellular histamine content was significantly increased 12 h after the addition of IgE. As prolonged treatment of BMMC with monomeric IgE has been reported to enhance the degree of degranulation by antigen stimulation (8), the increase in the amount of stored histamine by monomeric IgE in our study indicates that prolonged sensitization of mast cells with IgE may lead to an enhanced release of histamine. Regarding HDC protein expression in BMMCs, the 74-kD precursor form of HDC was the dominant form detected. We previously demonstrated that the 74-kD form of HDC is present in the cytosol as an enzymatically active form (18) and is degraded via the ubiquitin-proteasome pathway (23). In BMMCs treated with IgE, the rapid disappearance of the 74-kD form may be due to its rapid degradation via the ubiquitin–proteasome system.

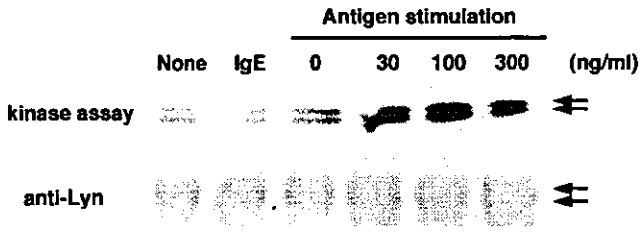

Figure 4. Absence of enzymatic activation of Lyn upon treatment with IgE. Enzymatic activation of Lyn following IgE sensitization was measured. BMMCs were incubated with anti-DNP IgE (IgE, 3 μg/ml) for 5 min. In the experiment of antigen stimulation, cells were sensitized with anti-DNP IgE (1 μg/ml) for 12 h and then incubated with DNP-human serum albumin (0, 30, 100, 300 ng/ml) for 5 min. In vitro kinase assay using [γ-^{32}P]ATP was performed as described in Materials and Methods. Immunoblot analyses were also performed using an anti-Lyn antibody (1:200) to confirm an equal amount of precipitated Lyn. The arrows indicate Lyn tyrosine kinase, which is detected as two bands with molecular mass of 53 and 56 kD.

Our results showing the lack of an increase in HDC expression in the absence of extracellular Ca^{2+} indicate that the induction of HDC requires the influx of extracellular Ca^{2+}. Indeed, addition of IgE to BMMCs caused a significant increase in cytoplasmic Ca^{2+}. Although such a sustained increase of cytosolic Ca^{2+} has previously been reported (9), it has been unclear as to which signaling pathway is involved in this Ca^{2+} increase. In our experiments, a PLC inhibitor, U73122, completely inhibited the increase in cytosolic Ca^{2+}, indicating that PLC may be activated upon stimulation with IgE even in the absence of antigen. Although a slight increase in cytoplasmic Ca^{2+} by IgE was observed in the absence of extracellular Ca^{2+}, it is likely that the sustained influx of extracellular Ca^{2+} is essential for the induction of HDC by monomeric IgE. Recently, it has been reported that thapsigargin induces HDC in a mouse macrophage cell line, via the activation of extracellular signal–regulated kinase (ERK; reference 24). In this study, we also confirmed that A23187, TPA, and thapsigargin induce HDC activity in BMMCs. TPA was able to induce HDC activity, but the degree of induction was much lower than that induced by IgE. These observations suggest that the influx of extracellular Ca^{2+} may play a crucial role in the induction of HDC in addition to activation of PKC. Evaluation of the effects of various PKC inhibitors on the induction of HDC by IgE suggests that this induction may be mediated by Ca^{2+}-dependent PKC, as Gö6976 has been reported to be a selective inhibitor for

Ca^{2+}-dependent PKC isozymes (25). However, as the other PKC inhibitors, such as bisindolylmaleimide and Ro-32-0432, were found to be ineffective, we cannot exclude the possibility that another PKC-like kinase is involved in the induction of HDC.

IL-6 production induced by monomeric IgE has been found to be inhibited by a PI-3 kinase inhibitor, LY294002, a MEK inhibitor, PD98059, and a p38 inhibitor, SB203580 (10). Although we have also observed these inhibitory effects on the IL-6 production under similar conditions to the previous report (3 μg/ml IgE, 3 h, control; 5.47 ± 0.634, + LY294002; 0 ± 0, + PD98059; 1.06 ± 0.164, + SB203580; 1.40 ± 0.193 ng/10^6 cells, n = 6), HDC induction by IgE was not suppressed by these inhibitors. These results indicate that signaling pathways involved in the induction of HDC and IL-6 are different, although both genes are induced by monomeric IgE in BMMCs. Induction of histamine synthesis in BMMCs was also found to be stimulated by antigen stimulation, as well as IL-6 production is. It remains to be clarified as to why histamine synthesis and IL-6 production is induced via IgE both in the presence and absence of antigen. One possible explanation is that the two pathways of HDC induction may occur in a different context of mast cell differentiation.

The partial suppression of HDC induction by herbimycin A and by PP2 indicates the involvement of Src family tyrosine kinases including Lyn, although stimulation with IgE did not augment the enzymatic activity of Lyn. This observation suggests that Src family tyrosine kinase other than Lyn may be involved in the induction of HDC. The inhibitory effect of a PLC inhibitor, U73122, indicates that PLC may be involved in the increase in cytosolic Ca^{2+} by IgE, although the signaling pathway responsible for the activation of PLC remains unknown. Further analyses on the pathways downstream of FcεRI activation, including the identification of the PKC isozyme activated by monomeric IgE, should be required.

In summary, we have demonstrated that monomeric IgE can induce histamine synthesis in BMMCs in the absence of its antigen. This induction requires the influx of extracellular Ca^{2+} and may be mediated by PKC.

We thank Ms A. Popiel for her help in preparation of the manuscript.

This study was supported by grants-in-aid for Scientific Research from the Ministry of Education, Science, Sports and Culture, Japan.

Submitted: 7 December 2001
Revised: 20 May 2002
Accepted: 13 June 2002

References

1. Metcalfe, D.D., D. Baram, and Y.A. Mekori. 1997. Mast cells. *Physiol. Rev.* 77:1033–1079.
2. Costa, J.J., P.F. Weller, and S.J. Galli. 1997. The cells of the allergic response. Mast cells, basophils, and eosinophils. *JAMA.* 278:1815–1822.
3. Mekori, Y.A., and D.D. Metcalfe. 2000. Mast cells in innate immunity. *Immunol. Rev.* 173:131–140.
4. Kinet, J.-P. 1999. The high-affinity IgE receptor (FcεRI): from physiology to pathology. *Annu. Rev. Immunol.* 17:931–972.
5. Furuichi, K., J. Rivera, and C. Isersky. 1985. The receptor for immunoglobulin E on rat basophilic leukemia cells: effect of ligand binding on receptor expression. *Proc. Natl. Acad. Sci. USA.* 82:1522–1525.
6. Quarto, R., J.-P. Kinet, and H. Metzger. 1985. Coordinate synthesis and degradation of the alpha-, beta- and gamma-subunit of the receptor for immunoglobulin E. *Mol. Immunol.* 22:1045–1051.
7. Hsu, C., and D. MacGlashan, Jr. 1996. IgE antibody up-regulates high affinity IgE binding on murine bone marrow derived mast cells. *Immunol. Lett.* 52:129–134.
8. Yamaguchi, M., C.S. Lantz, H.C. Oettgen, I.M. Katona, T. Fleming, K. Yano, I. Miyajima, J.-P. Kinet, and S.J. Galli. 1997. IgE enhances mouse mast cell FcεRI expression in vitro and in vivo: evidence for a novel amplification mechanism in IgE-dependent reactions. *J. Exp. Med.* 185:663–672.
9. Huber, M., C.D. Helgason, J.E. Damen, L. Liu, R.K. Humphries, and G. Krystal. 1998. The src homology 2-containing inositol phosphatase (SHIP) is the gatekeeper of mast cell degranulation. *Proc. Natl. Acad. Sci. USA.* 95:11330–11335.
10. Kalesnikoff, J., M. Huber, V. Lam, J.E. Damen, J. Zhang, R.P. Shiraganian, and G. Krystal. 2001. Monomeric IgE stimulates signaling pathways in mast cells that lead to cytokine production and cell survival. *Immunity.* 14:801–811.
11. Asai, K., J. Kitaura, Y. Kawakami, N. Yamagata, M. Tsai, D.P. Carbone, F. Liu, S.J. Galli, and T. Kawakami. 2001. Regulation of mast cell survival by IgE. *Immunity.* 14:791–800.
12. Ohmori, E., T. Fukui, N. Imanishi, K. Yatsunami, and A. Ichikawa. 1990. Purification and characterization of L-histidine decarboxylase from mouse mastocytoma P-815 cells. *J. Biochem.* 107:834–839.
13. Yamamoto, J., K. Yatsunami, E. Ohmori, Y. Sugimoto, T. Fukui, T. Katayama, and A. Ichikawa. 1990. cDNA-derived amino acid sequence of L-histidine decarboxylase from mouse mastocytoma p-815 cells. *FEBS Lett.* 276:214–218.
14. Ring, J., T. Senter, R.C. Cornell, C.M. Arroyave, and E.M. Tan. 1979. Plasma complement and histamine changes in atopic dermatitis. *Br. J. Dermatol.* 100:521–530.
15. Ring, J. 1983. Plasma histamine concentrations in atopic eczema. *Clin. Allergy.* 13:545–552.
16. Asahara, M., S. Musiake, S. Shimada, H. Fukui, Y. Kinoshita, C. Kawanami, T. Watanabe, S. Tanaka, A. Ichikawa, Y. Uchiyama, et al. 1996. Reg gene expression is increased in rat gastric enterochromaffin-like cells following water immersion stress. *Gastroenterology.* 111:45–55.
17. Rottem, M., J.P. Goff, J.P. Albert, and D.D. Metcalfe. 1993. The effects of stem cell factor on the ultrastructure of FcεRI$^+$ cells developing in IL-3-dependent murine bone marrow-derived cell cultures. *J. Immunol.* 151:4950–4963.
18. Tanaka, S., K. Nemoto, E. Yamamura, and A. Ichikawa. 1998. Intracellular localization of the 74- and 53-kDa forms of L-histidine decarboxylase in a rat basophilic/mast cell line, RBL-2H3. *J. Biol. Chem.* 273:8177–8182.
19. Grynkiewicz, G., M. Penie, and R.Y. Tsien. 1985. A new generation of Ca^{2+} indicators with greatly improved fluorescence properties. *J. Biol. Chem.* 260:3440–3450.

20. Takizawa, F., M. Adamczewski, and J.-P. Kinet. 1992. Identification of the low affinity receptor for immunoglobulin E on mouse mast cells and macrophages as FcγRII and FcγRIII. *J. Exp. Med.* 176:469–476.
21. Ujike, A., Y. Ishikawa, M. Ono, T. Yuasa, T. Yoshino, M. Fukumoto, J.V. Ravetch, and T. Takai. 1999. Modulation of immunoglobulin (Ig)E-mediated systemic anaphylaxis by low-affinity Fc receptors for IgG. *J. Exp. Med.* 189:1573–1579.
22. Turner, H., and J.-P. Kinet. 1999. Signaling through the high-affinity IgE receptor FcεRI. *Nature.* 402:B24–B30.
23. Tanaka, S., K. Nemoto, E. Yamamura, S. Ohmura, and A. Ichikawa. 1997. Degradation of the 74 kDa form of L-histidine decarboxylase via the ubiquitin-proteasome pathway in a rat basophilic/mast cell line (RBL-2H3). *FEBS Lett.* 417: 203–207.
24. Shiraishi, M., N. Hirasawa, Y. Kobayashi, S. Oikawa, A. Murakami, and K. Ohuchi. 2000. Participation of mitogen-activated protein kinase in thapsigargin- and TPA-induced histamine production in murine macrophage RAW264.7 cells. *Br. J. Pharmacol.* 129:515–524.
25. Martiny-Baron, G., M.G. Kazanietz, H. Mischak, P.M. Blumberg, G. Kochs, H. Hug, D. Marme, and C. Schachtele. 1993. Selective inhibition of protein kinase C isozymes by the indolocarbazole Go 6976. *J. Biol. Chem.* 268:9194–9197.

[CANCER RESEARCH 62, 28–32, January 1, 2002]

Advances in Brief

Involvement of Prostaglandin E Receptor Subtype EP_4 in Colon Carcinogenesis[1]

Michihiro Mutoh,[2] Kouji Watanabe,[2] Tomohiro Kitamura, Yutaka Shoji, Mami Takahashi, Toshihiko Kawamori, Kousuke Tani, Michiyoshi Kobayashi, Takayuki Maruyama, Kaoru Kobayashi, Shuichi Ohuchida, Yukihiko Sugimoto, Shuh Narumiya, Takashi Sugimura, and Keiji Wakabayashi[3]

Cancer Prevention Division, National Cancer Center Research Institute, Tokyo 104-0045, Japan [M. M., K. Wat., T. Kit., Y. S., M. T., T. Kaw., T. S., K. Wak.]; Minase Research Institute, Ono Pharmaceutical Co. Ltd., Osaka 618-8585, Japan [K. T., M. K., T. M., K. K., S. O.]; Department of Physiological Chemistry, Faculty of Pharmaceutical Sciences, Kyoto University, Kyoto 606-8315, Japan [Y. S.]; and Department of Pharmacology, Faculty of Medicine, Kyoto University, Kyoto 606-8315, Japan [S. N.]

Abstract

Accumulating evidence indicates that overproduction of prostanoids attributable to overexpression of cyclooxygenase-2 (COX-2) plays an important role in colon carcinogenesis. We have shown recently that the prostaglandin (PG) E receptor, EP_1, but not EP_3, is involved in mouse colon carcinogenesis. In line with our previous study, here we examined the role of prostanoid receptors in colon carcinogenesis using six additional lines of knockout mice deficient in prostanoid receptors EP_2, EP_4, DP, FP, IP, or TP. The animals were treated with the colon carcinogen, azoxymethane (AOM), and examined for the development of aberrant crypt foci (ACFs), putative preneoplastic lesions in the colon. Formation of ACFs was decreased only in the EP_4-knockout mice, to 56% of the wild-type level. To confirm these results, we also examined the inhibitory effects of an EP_4-selective antagonist, ONO-AE2–227, in the diet on the formation of AOM-induced colon ACFs in C57BL/6Cr mice and on the development of intestinal polyps in Min mice. ONO-AE2–227 at a dose of 400 ppm reduced the formation of ACFs to 67% of the control level, and intestinal polyp numbers in Min mice receiving 300 ppm were decreased to 69% of the control level. Plating efficiency assays showed that addition of 1.0 μM ONO-AE1–329, an EP_4-selective agonist, resulted in a 1.8-fold increase in the colony number of the human colon cancer cell line, HCA-7, similar to the effect of PGE_2. Moreover, EP_4 mRNA expression was clearly observed in normal colon mucosa and colon tumors in mice. Our previous and present results indicate that PGE_2 contributes to colon carcinogenesis through its actions mediated through EP_1 and EP_4 receptors; therefore, antagonists for these two receptors may be good candidates as chemopreventive agents against colon cancer.

Introduction

Clear benefits have been reported with NSAIDs[4] as chemopreventive agents against colon carcinogenesis (1, 2). NSAIDs inhibit arachidonic acid metabolism via actions on COX, a rate-limiting enzyme in the synthesis of PGs, which affect cell proliferation, tumor growth, apoptosis, and immune responsiveness. The presence of two isoforms of COX has been demonstrated—a constitutive enzyme, COX-1, and an inducible enzyme, COX-2—and a number of observations have suggested that increased activity of this latter plays a critical role in colon carcinogenesis (1–6). Recently, it was reported that genetic disruption of *COX-1*, as well as of *COX-2*, significantly reduces intestinal polyp formation in Min mice having a nonsense mutation in the *Apc* gene (7), so that COX-1 is also suggested to be involved in colon carcinogenesis to some extent.

When considering the possible mechanisms for the chemoprevention of colorectal cancer by NSAIDs, account must be taken of possible PG-independent mechanisms. Studies have shown that NSAIDs cause an increase in cellular arachidonic acid and stimulate the production of sphingomyelinase, resulting in hydrolysis of sphingomyelin to ceramide, which promotes apoptosis of tumor cells (8). Recently, the potential involvement of peroxisome proliferator-activated receptor δ as a adenomatous polyposis coli-regulated target of NSAIDs in colon cancer was demonstrated (9). Moreover, NSAIDs can up-regulate the *prostate apoptosis response 4* gene, a proapoptotic gene, in human colon carcinoma HCA-7 cells (10).

On the other hand, the most striking chemopreventive effects of NSAIDs are thought to be attributable to inhibition of COX with a resultant decrease in PG production. However, it is not fully clear what the legitimate molecular target of PGs is. Prostanoids such as PGE_2, PGD_2, $PGF_{2\alpha}$, PGI_2 and thromboxane A_2 exert their biological actions through binding to eight specific membrane receptors; the four subtypes EP_1 to EP_4 for PGE_2; DP for PGD_2; FP for $PGF_{2\alpha}$; IP for PGI_2; and TP for thromboxane A_2 (11, 12). The recent establishment of mice lacking the genes encoding these receptors (13–18) has enhanced our understanding of the involvement of prostanoids and their receptors in the development of colon cancer. In previous studies (19, 20), we demonstrated that PGE_2 contributes to colon carcinogenesis through its binding to the PGE_2 receptor subtype EP_1, using a genetic approach in EP_1-knockout mice and a pharmacological assessment with the EP_1-selective antagonists, ONO-8711 and ONO-8713. The same approach using EP_3-knockout mice indicated that the deficiency of EP_3 receptor has no effect on colon carcinogenesis (19).

The present study was conducted to examine the development of ACFs in six additional lines of mice lacking EP_2, EP_4, DP, FP, IP, or TP. Our results indicate a requirement for the EP_4 receptor in ACF formation by AOM. To confirm these data, we also examined the inhibitory effects of an EP_4-selective antagonist on the formation of colon ACFs induced by AOM in C57BL/6Cr mice and on the development of intestinal polyps in Min mice. Moreover, we determined EP_4 mRNA expression in colonic tissues of mice and examined cell proliferative effects of EP_4 receptor activation using an EP_4-selective agonist. On the basis of the results obtained, the role of EP_4 receptor in colon carcinogenesis is discussed.

Materials and Methods

Animals. Male C57BL/6Cr mice were purchased from Japan SLC, Inc. (Shizuoka, Japan) at 5 weeks of age and female C57BL/6J-Min/+ mice (Min mice) from The Jackson Laboratory (Bar Harbor, ME) at 6 weeks of age. The

Received 9/21/01; accepted 11/15/01.

The costs of publication of this article were defrayed in part by the payment of page charges. This article must therefore be hereby marked *advertisement* in accordance with 18 U.S.C. Section 1734 solely to indicate this fact.

[1] This work was supported in part by a grant from the Organization for Pharmaceutical Safety and Research of Japan, a Grant-in-Aid for Cancer Research and a Grant-in-Aid for the Second-Term Comprehensive 10-Year Strategy for Cancer Control from the Ministry of Health, Labor and Welfare of Japan, and a Grant-in-Aid for Scientific Research from the Ministry of Education, Science, Sports, Culture and Technology of Japan.

[2] These two authors contributed equally to this work.

[3] To whom requests for reprints should be addressed, at Cancer Prevention Division, National Cancer Center Research Institute, 1-1, Tsukiji 5-chome, Chuo-ku, Tokyo 104-0045, Japan. Phone: 81-3-3542-2511, extension 4500; E-mail: kwakabay@gan2.ncc.go.jp.

[4] The abbreviations used are: NSAID, nonsteroidal anti-inflammatory drug; COX, cyclooxygenase; PG, prostaglandin; ACF, aberrant crypt focus; AOM, azoxymethane; ONO-AE2–227, 2-[2-{2-(1-naphthyl)propanoylamino}phenyl]methylbenzoic acid; ONO-AE1–329, 16-(3-methoxymethyl)phenyl-ω-tetranor-3,7-dithia-PGE_1; cAMP, cyclic AMP; FBS, fetal bovine serum; RT-PCR, reverse transcription-PCR.

mouse genes encoding each of the six prostanoid receptors, EP_2, EP_4, DP, FP, IP, and TP, were disrupted by a gene knockout method using homologous recombination, as reported previously (13, 15–18). The generated chimeric mice were mated with C57BL/6Cr mice to produce heterozygotes for the respective alleles. The heterozygotes were backcrossed with C57BL/6Cr mice to exclude possible effects of genetic background. The resulting heterozygous male mice were intercrossed, and the F_2 progeny of the wild-type and homozygous mutant mice were used at 9 (EP_2, FP, IP, and TP) or 13 (DP) weeks of age. In the case of the EP_4-knockout mice, chimeric mice were mated to C57BL/6Cr mice, and homozygous mutants were obtained by interbreeding of the resulting agouti offspring. Most EP_4-deficient neonates with 129 × C57BL background become lethargic within 72 h after birth because of a patent ductus arteriosus, and <5% survive and grow normally (16). We used male EP_4-knockout mice that survived for analysis of ACF formation starting at 7 weeks of age. Genotypes of the knockout mice were confirmed by PCR according to the method described previously (13, 15–18). The animals were housed in plastic cages at 24 ± 2°C and 55% relative humidity with a 12/12-h light/dark cycle. Water and basal diet (AIN-76A; Bio-Serv, Frenchtown, NJ) or experimental diets, with addition of an EP_4-selective antagonist at the indicated concentrations with thorough mixing, prepared every week, were given *ad libitum*. Body weights and food intake were measured weekly. The experimental protocol was approved by the Institutional Ethics Review Committee for animal experimentation.

AOM-induced ACF Formation in Prostanoid Receptor-Knockout Mice. EP_2, EP_4, DP, FP, IP, and TP-knockout [$EP_2^{-/-}$ (male, n = 7), $EP_4^{-/-}$ (male, n = 10), $DP^{-/-}$ (female, n = 11), $FP^{-/-}$ (male, n = 9), $IP^{-/-}$ (male, n = 10), and $TP^{-/-}$ (male, n = 11)] mice and counterpart wild-type mice (n = 7–11/group) were treated with AOM (Sigma Chemical Co., St. Louis, MO) at a dose of 10 mg/kg body weight i.p. once a week for 3 weeks. All mice were sacrificed 5 weeks after the first dose of AOM. After laparotomy, the entire colons were resected and filled with 10% neutral buffered formalin and then opened longitudinally from the anus to the cecum. Each was fixed flat between sheets of filter paper in 10% neutral buffered formalin and then stained with 0.2% methylene blue in saline and scored under a light microscope for the number of ACFs/colon, number of ACs/colon, and mean number of ACs/focus according to the procedure of Bird (21).

The Selective EP_4 Antagonist, ONO-AE2–227. The selective EP_4 receptor antagonist, ONO-AE2–227, was chemically synthesized at Ono Pharmaceutical Co., Ltd. Receptor binding experiments with this compound were conducted using Chinese hamster ovary cell lines, stably expressing each type of mouse prostanoid receptor. The *Ki* values were found to be 2.7 nM for the mouse EP_4 receptor and 21 nM for mouse EP_3 receptor. The *Ki* values for the other receptors, mouse EP_1, EP_2, DP, FP, IP, and TP receptors were >1000 times higher than that for the mouse EP_4 receptor. Analysis of its agonistic and antagonistic actions showed the compound to act as a potent and competitive antagonist to the EP_4 receptor; it inhibited PGE_2 (100 nM)-induced increase in cytosolic cAMP concentration with a median inhibitory concentration of 10 nM. ONO-AE2–227 also acted as a relatively weak antagonist to the EP_3 receptor; it inhibited the PGE_2 (10 nM)-induced increase in cytosolic calcium concentration with an IC_{50} of 160 nM. Details for the chemical synthesis and biological activities of ONO-AE2–227 will be reported elsewhere. By high performance liquid chromatography, ONO-AE2–227 was confirmed to be stable for at least 4 weeks at ambient temperature in the diet.

Effects of ONO-AE2–227 on Formation of AOM-induced ACF in C57BL/6Cr Mice and Intestinal Polyps in Min Mice. C57BL/6Cr male mice, 6 weeks of age, were given i.p. injections of AOM or the vehicle, as described in the experiments for the different lines of prostanoid receptor-knockout mice. The mice in the EP_4-selective antagonist-treated groups were fed diets containing 100 or 400 ppm of ONO-AE2–227 starting the day before the first AOM dosing until the end of the experiment at week 5. Numbers of AOM-injected mice were eight for each group, and those for vehicle-injected mice were three for the 400 ppm of experimental diet groups and three for the control diet group. ACF in the colon of mice were assessed as described above.

Groups of 10 female Min mice were fed diet containing ONO-AE2–227 or basal diet from 6 weeks of age until the termination of the experiment 7 weeks thereafter. It is expected that C57BL/6Cr mice are generally much resistant to chemical treatment than Min mice. In addition, the experimental period with Min mice was longer than that of ACF induction in the experiment with C57BL/6Cr. Therefore, the dose of 300 ppm of ONO-AE2–227 was chosen for the experiment. After sacrifice and laparotomy, the entire intestinal tract was resected, filled with 10% neutral buffered formalin, and divided into four sections: the colon and three sections of the small intestine, including the proximal (~4 cm from the pylorus ring of stomach), middle (the proximal half of the remainder), and distal parts. These sections were opened longitudinally and fixed flat between sheets of filter paper in 10% neutral buffered formalin, and the numbers and sizes of polyps were determined under a stereoscopic microscope.

Effects of ONO-AE1–329 and PGE_2 on Colony Formation of HCA-7 Cells. HCA-7 colony 29, a human colon adenocarcinoma cell line, was kindly provided from Dr. Susan Kirkland (Imperial College of Science, Technology and Medicine, London, United Kingdom). The cells were maintained in DMEM supplemented with 10% heat-inactivated FBS (Hyclone Laboratories, Inc., Logan, UT) and antibiotics (100 μg/ml of streptomycin and 100 units/ml of penicillin) at 37°C in 5% CO_2. The numbers of HCA-7 cell colonies were counted as described previously (22) with slight modifications. In brief, HCA-7 cells were plated in 6-cm cell culture dishes at a density of 1000 cells/dish, with DMEM containing 10% FBS. The selective EP_4 receptor agonist, ONO-AE1–329 (23), or PGE_2 (Cayman Chemical Co., MI) was added daily to selected cells, and the medium was also replaced every day. Cells were incubated for 14 days, and then colonies were visualized by staining with 0.2% methylene blue and counted manually.

Analysis of EP_4 Expression by RT-PCR in Colon Cancer Samples from AOM-treated Mice. Male C57BL/6J mice (CLEA Japan, Inc., Tokyo, Japan) at 7 weeks of age were i.p. injected with 10 mg/kg body weight of AOM once a week for a total of six times to obtain many colon tumors, as described previously (3), and sacrificed at 50 weeks after the first injection. Their colons were removed, and one half of each of five colon tumors and five neighboring normal mucosa samples were immediately frozen, stored at −80°C, and used for RT-PCR analyses. The samples were sonicated, and total RNAs were isolated using ISOGEN (Nippon Gene Co., Tokyo, Japan). One-μg aliquots of total RNA were subjected to the reverse transcription reaction using an RNA LA PCR kit (Takara Shuzo Co., Shiga, Japan). Oligonucleotide primers specific for mouse EP_4 (5′-TTCCGCTCGTGGTGCGAGTGTTC-3′; 5′-GAGGTGGTGTCTGCTTGGGTCAG-3′) were used for amplification of each mRNA. All PCR reactions were performed in a final volume of 50 μl for 30 cycles. The PCR products were analyzed by 2% agarose gel electrophoresis.

Statistical Analysis. The data for ACF and polyp formation are expressed as mean ± SE, and their statistical analysis was carried out with the Student's t test. Differences were considered statistically significant at $P < 0.05$.

Results

ACF Development in Prostanoid Receptor-Knockout Mice. To determine which prostanoid receptors might be involved in colon carcinogenesis, we used a short-term *in vivo* model using ACF formation induced by AOM as the end point. The mean body weights of the AOM-treated EP_4-knockout mice were comparable with those of AOM-treated wild-type mice. No abnormal clinical signs were observed during the course of the experiment, and no change was evident in organ weights including the liver, kidneys, and spleen between the two groups. ACFs were noted in all animals treated with AOM and were located mainly in the distal colon, with fewer numbers in the middle colon and rectum. In wild-type ($EP_4^{+/+}$, n = 10) and knockout ($EP_4^{-/-}$, n = 10) mice, the numbers of ACFs/colon were 14.6 ± 2.0 and 8.2 ± 1.4 ($P < 0.05$), and the mean numbers of ACs/focus were 1.5 ± 0.1 and 1.5 ± 0.1, respectively. Thus, the numbers of ACFs per colon in EP_4-knockout mice were significantly reduced to 56% of the wild-type value. Mice treated with saline showed no evidence of ACF formation in either knockout or wild-type mice.

Under the same conditions, the effects of deficiency of EP_2, DP, FP, IP, or TP receptors on formation of ACFs were examined. As with the EP_4-knockout mice, no abnormal changes in body or organ weights were observed in knockout mice compared with wild-type mice, except for a slight increase in spleen weights of IP-knockout mice. There were no significant differences in the numbers of ACFs/

colon in EP_2, DP, FP, IP, and TP-knockout mice from those of their wild-type counterparts. Moreover, the mean numbers of ACs/focus in these receptor-knockout mice groups did not differ from those in the wild-type mice. Fig. 1 summarizes the data for the effects of six prostanoid receptor deficiencies on AOM-induced ACF in mice. For reference, the results for EP_1- and EP_3-knockout mice, reported previously (19), are also included in Fig. 1.

Suppression of AOM-induced ACF Formation by the EP_4-selective Antagonist in C57BL/6Cr Mice. To confirm a role for the EP_4 receptor in colon carcinogenesis, we investigated the effects of ONO-AE2–227, a selective EP_4 antagonist, on the formation of ACF induced by AOM in C57BL/6Cr mice. Administration of diet containing 100 or 400 ppm of ONO-AE2–227 did not affect the body and organ weights in the AOM-injected groups. ACFs were observed in all animals ($n = 8$ for each group) treated with AOM. Administration of 400 ppm of ONO-AE2–227 to AOM-treated mice throughout the experiment for 5 weeks significantly decreased the numbers of ACFs/colon (8.3 ± 1.1, $P < 0.05$) to 67% of that (12.4 ± 2.0) for the AOM-alone group. The mean numbers of ACs/focus in the two groups were both 1.5 ± 0.1. The numbers of ACFs/colon and the mean numbers of ACs/focus in 100 ppm of the ONO-AE2–227 group were 12.4 ± 1.6 and 1.5 ± 0.1, respectively. Thus, administration of 100 ppm of ONO-AE2–227 did not affect ACF formation. No ACFs were observed in vehicle-injected mice, with or without 400 ppm ONO-AE2–227.

Suppression of Intestinal Polyp Formation by the EP_4-selective Antagonist in Min Mice. Administration of ONO-AE2–227 at a dose of 300 ppm in the diet for 7 weeks did not affect the body weights, feeding, or behavior of Min mice. Data for number and distribution of intestinal polyps in the basal diet and ONO-AE2–227 groups are shown in Table 1. Most polyps were located in the small intestine with only a few in the colon. Administration of ONO-AE2–227 significantly reduced the total number of polyps to 69% of that in the basal diet group. The number of polyps detected in the distal portion of the small intestines was significantly lower (65% of the basal diet group value), and that in the middle portion was also lower (74% of the basal diet group value), although this was not statistically significant. Fig. 2 shows the size distributions of intestinal polyps in the basal diet and ONO-AE2–227-treated groups. Treatment with the EP_4-selective antagonist significantly reduced the number of polyps measuring ≥1.0 mm in diameter but not those measuring <1.0 mm in diameter.

Table 1 *Suppression of intestinal polyp development by ONO-AE2-227 in Min mice*

Mice were fed basal diet or diet containing 300 ppm of ONO-AE2-227 for 7 weeks. Numbers of Min mice fed the experimental and control diets were ten each. Data are mean ± SE. Numbers in parentheses indicate percentage compared with the basal diet group.

Polyp location	No. of polyps/mouse	
	Basal diet	ONO-AE2-227
Proximal small intestine	4.0 ± 0.4	3.3 ± 1.1 (83)
Middle small intestine	19.3 ± 2.0	14.2 ± 2.2 (74)
Distal small intestine	37.6 ± 5.3	24.5 ± 2.0[a] (65)
Colon	0.5 ± 0.2	0.2 ± 0.1 (40)
Total	61.4 ± 7.3	42.2 ± 4.3[a] (69)

[a] $P < 0.05$ *versus* the basal diet group.

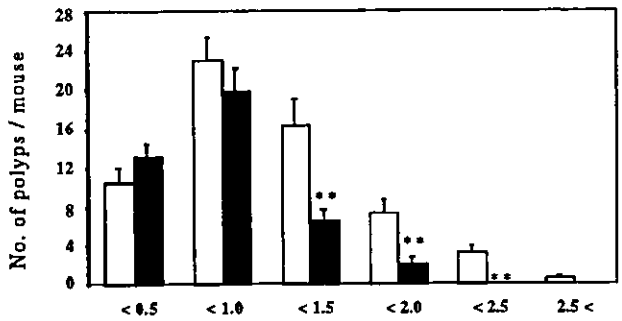

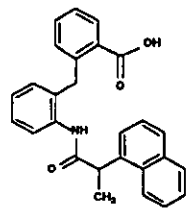

ONO-AE2-227

Fig. 2. Size distribution of intestinal polyps in Min mice. □, basal diet; ■, 300 ppm ONO-AE2–227. (The structure is shown in *lower part* of the figure). Polyps were classified in terms of their diameters in millimeters. The number of polyps/mouse in each size class is expressed as the means; *bars*, SE. **, $P < 0.01$, compared with the basal diet group.

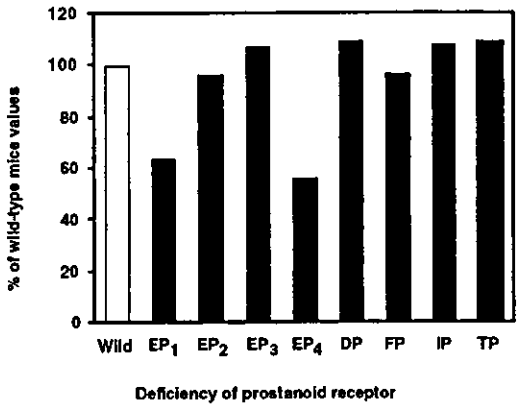

Fig. 1. Numbers of ACFs developing in the colons of prostanoid receptor-knockout mice and their wild-type counterparts after treatment with AOM. EP_1, EP_2, EP_3, EP_4, DP, FP, IP, and TP-knockout mice and their respective wild-type mice were treated with AOM, and the numbers of ACFs were scored at 5 weeks after the first dose of AOM. The values (numbers of ACFs/colon) for each knockout mouse group are expressed as percentages of those for their wild-type counterparts. The data for EP_1- and EP_3-knockout mice are from our previously published work (19). □, wild-type mice; ■, knockout mice. *, $P < 0.05$, compared with the wild-type mice.

Effects of the EP_4-Selective Agonist and PGE_2 Treatment on Colony Formation of HCA-7 Cells. To evaluate the physiological functions of the EP_4 receptor, we examined the effects of the EP_4 receptor-selective agonist, ONO-AE1–329, and PGE_2 treatment on colony formation in monolayer cultures. We used a human colon epithelial cell line, HCA-7 cells, in which expression of the EP_4 receptor could be detected by RT-PCR analysis (data not shown). For this experiment, 1000 cells were seeded in six-cm dishes, and ONO-AE1–329 was added daily at concentrations of 0.1, 1.0, and 10 μM in fresh medium for 14 days. We observed a 1.8-fold increase in HCA-7 colony number in the presence of 1.0 μM ONO-AE1–329 and a 1.5-fold increase in the presence of 1.0 μM PGE_2 for 14 days (Fig. 3). The highest dose of ONO-AE1–329 (10 μM) decreased the HCA-7 colony number.

EP_4 mRNA Expression in Normal Colon and Colon Cancer Tissues in Mice. The expression of EP_4 mRNA in normal colon mucosal and tumor tissues from five mice was examined. Representative data are shown in Fig. 4. EP_4 mRNA was detected in all colon tumor and normal mucosa samples by RT-PCR. All of the tumors

sampled were histopathologically diagnosed as well-differentiated adenocarcinomas.

Discussion

In the present study, examination of the effects of EP_2, EP_4, DP, FP, IP, and TP receptor knockout on AOM-induced ACF formation in mice provided evidence for the involvement of the PGE_2 receptor subtype EP_4 but not EP_2, DP, FP, IP, or TP in colon carcinogenesis. In addition, administration of an EP_4-selective antagonist, ONO-AE2-227, to AOM-treated C57BL/6Cr mice and Min mice decreased ACFs and intestinal polyp formation, respectively. Interestingly, in the latter case the number of polyps $\geq$1.0 mm in diameter, but not those <1.0 mm in diameter, were reduced, suggesting reduction in tumor growth. An EP_4-selective agonist, ONO-AE1-329, was further found to increase colony formation by HCA-7 cells, similar to PGE_2. Moreover, we could demonstrated the expression of EP_4 receptors in colon tumors and normal mucosa, in line with earlier results of *in situ* hybridization for EP_4 mRNA (24). In the previous study, EP_1 receptor was shown to be involved in colon carcinogenesis (19). In addition, our preliminary study indicated that EP_1 receptor expression was detected in AOM-induced colon tumors in mice by RT-PCR analysis (data not shown). Thus, combined together, our present and previous results suggest that PGE_2 mediates carcinogenic changes by acting at EP_1 and EP_4 receptors in the colon. Consistent with these data, increased PGE_2 levels in colon tumor tissues compared with the surrounding normal mucosa were suggested to play an important role in colon carcinogenesis (25).

PGE_2 was earlier suggested to stimulate an increase in cell proliferation and motility of the colon cancer cell line LS-174 by activating the phosphatidylinositol 3-kinase/Akt pathway via EP_4 receptor activation (26). It is also known that PGE_2 activates adenylate cyclase via a cholera toxin-sensitive, stimulatory G protein through binding to the EP_4 receptor. In the adenylate cyclase pathway, increased cAMP levels result in an activation of cAMP-dependent protein kinase (PKA) and a transcriptional factor that binds to cAMP-responsive elements to transactivate the transcription of specific primary response genes that initiate cell proliferation (27). These biological changes could contribute to colon carcinogenesis through EP_4 receptor involvement. The EP_1 receptor is a transmembrane G protein-coupled receptor, similar to other PGE_2 receptors, but its signal transduction mechanism is not known in detail. EP_1 signals are transmitted by increased intracellular Ca^{2+} concentrations and activate protein kinase C (11, 12). Additional studies are needed to investigate events downstream of the EP_1 receptor signaling pathway and any link between EP_1 and EP_4 receptors. Recently, it was reported that homozygous deletion of the gene encoding EP_2 receptor resulted in decrease of intestinal polyp formation in the *Apc* knockout mice (28). These data are not consistent with the results obtained in the present study. Therefore, involvement of EP_2 receptor in AOM-induced colon carcinogenesis in rodents and intestinal polyp formation in Min mice needs to be examined using EP_2 receptor antagonists.

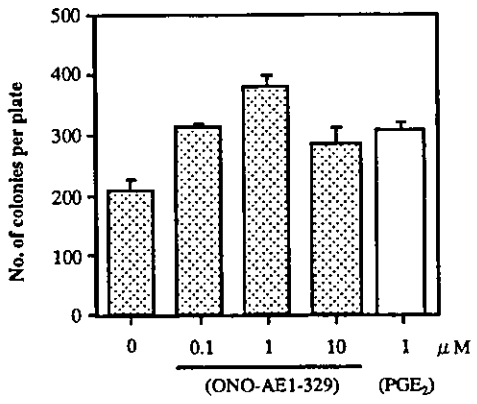

Fig. 3. HCA-7 colony number in response to treatment with ONO-AE1-329 or PGE_2. HCA-7 cells were plated in six-cm cell culture dishes at a density of 1000 cells/dish, with DMEM containing 10% FBS. Cells were incubated for 14 days, and then colonies were visualized by staining with 0.2% methylene blue and counted manually. Data are means (n = 3); *bars*, SE. Similar results were obtained in three separate experiments.

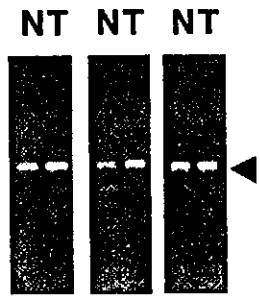

Fig. 4. EP_4 receptor expression in normal colon and colon cancer tissues of mice. Aliquots of total RNA (1 μg) from colon cancers and neighboring normal colon tissues were subjected to RT-PCR. The reaction mixture for mouse EP_4 was first heated at 94°C for 2 min, followed by amplification for 30 cycles at 95°C for 30 s, 60°C for 45 s, and 72°C for 4 min. These temperatures and time intervals were followed by a final incubation at 72°C for 5 min. The PCR products were separated on 2% agarose gels, and portions corresponding to the expected DNA size (488 bp) of the PCR products are shown in the *middle* of the figure with an *arrow*. *N*, normal mucosa; *T*, tumor.

Selective inhibitors of COX-2 are good candidates as chemopreventive agents, with clinically important mechanism-based safety characteristics that significantly distinguish them from traditional NSAIDs, which suffer from gastrointestinal side effects that limit long-term application. It might be expected that these adverse effects are further diminished by inhibiting the downstream of COX pathway. On the basis of the present results, selective EP_1 and/or EP_4 receptor antagonists may be particularly beneficial as chemopreventive agents for colon cancer with low toxicity.

In conclusion, the data obtained in our present and previous studies suggest that PGE_2 mediates colonic carcinogenic changes by acting at EP_1 and EP_4 receptors in the colon. For confirmation, long-term colon carcinogenesis experiments with EP_1 and EP_4 antagonists are currently being conducted in our laboratory.

References

1. Smalley, W. E., and DuBois, R. N. Colorectal cancer and nonsteroidal anti-inflammatory drugs. Adv. Pharmacol., *39:* 1–20, 1997.
2. Elder, D. J. E., and Paraskeva, C. COX-2 inhibitors for colorectal cancer. Nat. Med., *4:* 392–393, 1998.
3. Fukutake, M., Nakatsugi, S., Isoi, T., Takahashi, M., Ohta, T., Mamiya, S., Taniguchi, Y., Sato, H., Fukuda, K., Sugimura, T., and Wakabayashi, K. Suppressive effects of nimesulide, a selective inhibitor of cyclooxygenase-2, on azoxymethane-induced colon carcinogenesis in mice. Carcinogenesis (Lond.), *19:* 1939–1942, 1998.
4. Kawamori, T., Rao, C. V., Seibert, K., and Reddy, B. S. Chemopreventive activity of celecoxib, a specific cyclooxygenase-2 inhibitor, against colon carcinogenesis. Cancer Res., *58:* 409–412, 1998.
5. Steinbach, G., Lynch, P. M., Phillips, R. K., Wallace, M. H., Hawk, E., Gordon, G. B., Wakabayashi, N., Saunders, B., Shen, Y., Fujimura, T., Su, L. K., and Levin, B. The effect of celecoxib, a cyclooxygenase-2 inhibitor, in familial adenomatous polyposis. N. Engl. J. Med., *342:* 1946–1952, 2000.
6. Oshima, M., Dinchuk, J. E., Kargman, S. L., Oshima, H., Hancock, B., Kwong, E., Trzaskos, J. M., Evans, J. F., and Taketo, M. M. Suppression of intestinal polyposis in *Apc* $^{\Delta 716}$ knockout mice by inhibition of cyclooxygenase 2 (COX-2). Cell, *87:* 803–809, 1996.
7. Chulada, P. C., Thompson, M. B., Mahler, J. F., Doyle, C. M., Gaul, B. W., Lee, C., Tiano, H. F., Morham, S. G., Smithies, O., and Langenbach, R. Genetic disruption of *Ptgs-1*, as well as *Ptgs-2*, reduces intestinal tumorigenesis in Min mice. Cancer Res., *60:* 4705–4708, 2000.
8. Chan, T. A., Morin, P. J., Vogelstein, B., and Kinzler, K. W. Mechanisms underlying nonsteroidal antiinflammatory drug-mediated apoptosis. Proc. Natl. Acad. Sci. USA, *95:* 681–686, 1998.
9. He, T. C., Chan, T. A., Vogelstein, B., and Kinzler, K. W. PPARδ is an APC-regulated target of nonsteroidal anti-inflammatory drugs. Cell, *99:* 335–345, 1999.

10. Zhang, Z., and DuBois, R. N. *Par-4*, a proapoptotic gene, is regulated by NSAIDs in human colon carcinoma cells. Gastroenterology, *118:* 1012–1017, 2000.
11. Coleman, R. A., Smith, W. L., and Narumiya, S. International Union of Pharmacology classification of prostanoid receptors: properties, distribution, and structure of the receptors and their subtypes. Pharmacol. Rev., *46:* 205–229, 1994.
12. Ushikubi, F., Hirata, M., and Narumiya, S. Molecular biology of prostanoid receptors: an overview. J. Lipid Mediat. Cell Signalling, *12:* 343–359, 1995.
13. Matsuoka, T., Hirata, M., Tanaka, H., Takahashi, Y., Murata, T., Kabashima, K., Sugimoto, Y., Kobayashi, T., Ushikubi, F., Aze, Y., Eguchi, N., Urade, Y., Yoshida, N., Kimura, K., Mizoguchi, A., Honda, Y., Nagai, H., and Narumiya, S. Prostaglandin D_2 as a mediator of allergic asthma. Science (Wash. DC), *287:* 2013–2017, 2000.
14. Ushikubi, F., Segi, E., Sugimoto, Y., Murata, T., Matsuoka, T., Kobayashi, T., Hizaki, H., Tuboi, K., Katsuyama, M., Ichikawa, A., Tanaka, T., Yoshida, N., and Narumiya, S. Impaired febrile response in mice lacking the prostaglandin E receptor subtype EP_3. Nature (Lond.), *395:* 281–284, 1998.
15. Hizaki, H., Segi, E., Sugimoto, Y., Hirose, M., Saji, T., Ushikubi, F., Matsuoka, T., Noda, Y., Tanaka, T., Yoshida, N., Narumiya, S., and Ichikawa, A. Abortive expansion of the cumulus and impaired fertility in mice lacking the prostaglandin E receptor subtype EP_2. Proc. Natl. Acad. Sci. USA, *96:* 10501–10506, 1999.
16. Segi, E., Sugimoto, Y., Yamasaki, A., Aze, Y., Oida, H., Nishimura, T., Murata, T., Matsuoka, T., Ushikubi, F., Hirose, M., Tanaka, T., Yoshida, N., Narumiya, S., and Ichikawa, A. Patent ductus arteriosus and neonatal death in prostaglandin receptor EP_4-deficient mice. Biochem. Biophys. Res. Commun., *246:* 7–12, 1998.
17. Sugimoto, Y., Yamasaki, A., Segi, E., Tsuboi, K., Aze, Y., Nishimura, T., Oida, H., Yoshida, N., Tanaka, T., Katsuyama, M., Hasumoto, K., Murata, T., Hirata, M., Ushikubi, F., Negishi, M., Ichikawa, A., and Narumiya, S. Failure of parturition in mice lacking the prostaglandin F receptor. Science (Wash. DC), *277:* 681–683, 1997.
18. Murata, T., Ushikubi, F., Matsuoka, T., Hirata, M., Yamasaki, A., Sugimoto, Y., Ichikawa, A., Aze, Y., Tanaka, T., Yoshida, N., Ueno, A., Oh-ishi, S., and Narumiya, S. Altered pain perception and inflammatory response in mice lacking prostacyclin receptor. Nature (Lond.), *388:* 678–682, 1997.
19. Watanabe, K., Kawamori, T., Nakatsugi, S., Ohta, T., Ohuchida, S., Yamamoto, H., Maruyama, T., Kondo, K., Ushikubi, F., Narumiya, S., Sugimura, T., and Wakabayashi, K. Role of the prostaglandin E receptor subtype EP_1 in colon carcinogenesis. Cancer Res., *59:* 5093–5096, 1999.
20. Watanabe, K., Kawamori, T., Nakatsugi, S., Ohta, T., Ohuchida, S., Yamamoto, H., Maruyama, T., Kondo, K., Narumiya, S., Sugimura, T., and Wakabayashi, K. Inhibitory effect of a prostaglandin E receptor subtype EP_1 selective antagonist, ONO-8713, on development of azoxymethane-induced aberrant crypt foci in mice. Cancer Lett., *156:* 57–61, 2000.
21. Bird, R. P. Observation and quantification of aberrant crypts in the murine colon treated with a colon carcinogen: preliminary findings. Cancer Lett., *37:* 147–151, 1987.
22. Sheng, H., Shao, J., Morrow, J. D., Beauchamp, R. D., and DuBois, R. N. Modulation of apoptosis and Bcl-2 expression by prostaglandin E_2 in human colon cancer cells. Cancer Res., *58:* 362–366, 1998.
23. Yamane, H., Sugimoto, Y., Tanaka, S., and Ichikawa, A. Prostaglandin E_2 receptors, EP_2 and EP_4, differentially modulate TNF-α and IL-6 production induced by lipopolysaccharide in mouse peritoneal neutrophils. Biochem. Biophys. Res. Commun., *278:* 224–228, 2000.
24. Morimoto, K., Sugimoto, Y., Katsuyama, M., Oida, H., Tsuboi, K., Kishi, K., Kinoshita, Y., Negishi, M., Chiba, T., Narumiya, S., and Ichikawa, A. Cellular localization of mRNAs for prostaglandin E receptor subtypes in the mouse gastrointestinal tract. Am. J. Physiol, *272:* G681–G687, 1997.
25. Rigas, B., Goldman, I. S., and Levine, L. Altered eicosanoid levels in human colon cancer. J. Lab. Clin. Med., *122:* 518–523, 1993.
26. Sheng, H., Shao, J., Washington, M. K., and DuBois, R. N. Prostaglandin E_2 increases growth and motility of colorectal carcinoma cells. J. Biol. Chem., *276:* 18075–18081, 2001.
27. Dhanasekaran, N., Tsim, S. T., Dermott, J. M., and Onesime, D. Regulation of cell proliferation by G proteins. Oncogene, *17:* 1383–1394, 1998.
28. Sonoshita, M., Takaku, K., Sasaki, N., Sugimoto, Y., Ushikubi, F., Narumiya, S., Oshima, M., and Taketo, M. M. Acceleration of intestinal polyposis through prostaglandin receptor EP_2 in $Apc^{\Delta 716}$ knockout mice. Nat. Med., *7:* 1048–1051, 2001.